Peristaltic motion of Non-Newtonian fluid under the influence of inclined magnetic field, porous medium and chemical reaction

R. Vijayaragavan [1], P. Tamizharasi [1,] A. Magesh [2,*]

[1]Thiruvalluvar University, Serkadu,, Vellore, Tamilnadu, India – 632 115

[2]JEI Mathaajee College of Engineering, Kanchipuram, India 631 552.

([*]Corresponding Author: mageshmaths86@gmail.com)

Abstract

In this article, we studied the peristaltic motion of Jeffrey fluid with the porous medium through an asymmetric channel under the influence of velocity slip parameters. Governing equations for non-Newtonian fluid flow models, such as continuity, momentum, energy and mass transfer, are formulated. An externally applied inclined magnetic field is also considered in the flow pattern. The lengthy governing equation of fluid motion is reduced by considering the approximation of longer wavelengths and smaller Reynolds numbers. $(\mathrm{Re} \to 0)$. The resulting governing equations are solved exactly. The graph shows the results of the impact of various related fluid parameters such as Hartmann number, Darcy number, Jeffrey fluid parameter, amplitude ratio, chemical reactions of fluid velocity, temperature, concentration, pressure rise, pressure gradient, streamlines etc. Finally, the various waveforms of the trapping phenomenon are presented.

Key words: Inclined magnetic field, peristaltic transport, Porous medium, slip parameters

---

Present Address of the authors

Dr.R.Vijayaragavan,
Professor of Mathematics, Thiruvalluvar University, Serkadu, Vellore 632 115, India.

Dr.P.Tamizharasi,
Assistant Professor of Mathematics, Easwari Engineering College, Ramapuram, Chennai 600 089, India.

Dr.A.Magesh, Assistant Professor of Mathematics, Sri Sai Ram Engineering College, Chennai 600 044, India.

Nomenclature

Symbols

$\bar{h}_1, \bar{h}_2$ Upper and lower walls $[L]$

$u = (\hat{U}', \hat{V}')$ Velocity vector on $(\hat{X}', \hat{Y}')$ Direction

I Identity tensor

B_0 Magnetic field vector

T Temperature of fluid

S Cauchy stress tensor

d_1, d_2 Channel wall's constant height $[L]$

a_1, b_1 Wave amplitudes $[L]$

c Wave speed $[L/T]$

$\hat{t}'$ Time $[T]$

P Pressure $[ML/T^2]$

c_p Specific heat $[ML^2/T^2K]$

k_1 Permeability parameter

T_0, T_1 Temperature at lower and upper wall $[K]$

Re Reynolds number

Da Darcy number

Fr Frude number

Pr Prandtl number

M Hartmann number

E Eckert number

Br Brinkmann number

F Flow rate $[L^3/T]$

Greek symbols

λ_1, λ_2 Constants of Jeffrey fluid

$\dot{\gamma}, \ddot{\gamma}$ Shear stress

λ Wavelength $[L]$

ρ Density $[M/L^3]$

μ Dynamic viscosity

σ Electrical conductivity

δ Wave number

ψ Stream function

κ_t Thermal conductivity $[ML/T^3K]$

α Inclination angle

$\bar{\eta}_1, \bar{\eta}_2$ First, second order slip parameters

β^* Thermal slip parameter

γ_1 Chemical reaction Parameter

1. Introduction

The peristaltic movement of non-Newtonian and Newtonian fluids has received particular attention for its wide applications in physiology, engineering and modern industry. In physiological terms, urine transport to the bladder through the kidney, in the ingestion of food via the esophagus, capillaries and arterioles, vasomotion of venues, in the unsanitary transport of fluids, in the movement of worms, transport of toxic fluids in the nuclear industry, roller, finger pumps. Latham made the initial attempt at peristaltic transport [1]. Brown and

Hung [2] investigated non-linear two-dimensional peristaltic transportation using experimental and computational methods. The peristaltic movement through an inclined tube of Herschel-Bulkley fluid has been described by Vajravelu et al. [3]. Wang et al. [4] discussed the Johnson Segalman fluid through peristalsis in the deformable tube. A few studies on the peristaltic mechanism of different fluid patterns are presented [5-8].

The study of the peristaltic transport of MHD (magnetohydrodynamic) has special attention due to its numerous applications in electricity production, bio-engineering and medicine. In particular, blood pumps, generator sets, MHD compressor operation, flow meters, radar systems, heat exchanger construction, etc. MHD dust fluid through Peristaltic transport was described by Muthuraj et al. [9]. They employed an analytic solution to solve the equations of solids and liquids and reported that the appearance of magnetic parameters on the transverse side that creates the drag force and affects the movement of the liquid in the opposite direction, causing the velocity to decrease. A few studies of peristaltic motion with MHD in different fluids under different boundary conditions are presented [10-14].

Porous materials provide significant advantages in comparison with conventional construction. The non-uniform flow of fluids ensures that fluids are uniformly blended and also supports them in maintaining the temperature distribution. Mathematically, the flow rate in the porous medium is defined by Darcy's law [15]. He indicated that the flow rate is straightly proportional to pressure gradient and the flow cross-section. Some studies based on the presence of porous media across different fluid flow patterns in different flow geometries can be found in [16-25]. Nadeem et al. [26] Discussed the peristaltic movement of Jeffrey nanofluid in rectangular ducts. Blood clots are a major cause of various illnesses around the world, like heart attacks; stroke is the main element behind death, is addressed by Bhatti et al. [27]. Tripathi et al. [28] focused on the peristaltic movement of the micropolar liquid in an asymmetrical channel with electroosmosis. They used a numerical solution to obtain the solution. Magesh and Kothandapani [29] examined the power and mass transfer analysis of the Johnson Segalmann fluid in an asymmetric channel.

All studies above, but few in the available literature, on the impact of velocity second slip conditions on the peristaltic movement in a channel/tube. Granting to the available literature, no effort has been gained to influence of velocity second slip conditions through the peristaltic mechanism of Jeffrey fluid in an inclined asymmetric channel. Thus, the present study proposes to construct the work on the impact of velocity second slip parameters of the peristaltic movement of Jeffrey fluid. The flow is considered with porous medium, electrically conductive inclined magnetic field and chemical reaction. Mass and energy transfer of the fluid was also studied. The exact solutions are derived from the simplified governing

equations. The influence of various fluid parameters of the flow characteristics are analyzed by means of graphic illustrations.

2. Formulation of the present problem

We consider viscous, incompressible, unsteady two-dimensional Jeffrey fluid induced by a peristaltic system through an asymmetrical channel enclosed by $\bar{h}_1\left(\hat{X}',\hat{t}'\right)$ and $\bar{h}_2\left(\hat{X}',\hat{t}'\right)$. The fluid is considered to drive electrically in the appearance of an inclined magnetic field and porous medium. The flow generates sinusoidal waves propagating at a non-varying speed c through the channel walls. Asymmetry of the channel due to phase difference (see Fig.[1]) is represented by [30,31]

$$\bar{h}_1 = -d_2 - b_1 cos\left[\frac{2\pi\left(\hat{X}' - c\hat{t}'\right)}{\lambda} + \phi\right],$$

$$\bar{h}_2 = d_1 + a_1 cos\left[\frac{2\pi\left(\hat{X}' - c\hat{t}'\right)}{\lambda}\right], \tag{1}$$

Where $d_1 + d_2$, ϕ, a_1, b_1 are the channel width, phase difference and amplitudes of the waves. ϕ changes in the range $0 \le \phi \le \pi$, the channel is symmetric at $\phi = 0$ (waves out of phase) and the waves are in phase at $\phi = \pi$, λ is wave length and further b_1, a_1, d_2, d_1 and ϕ satisfies as the following relation is

$$b_1^2 + a_1^2 + 2b_1 a_1 \cos\phi \le (d_2 + d_1)^2 \tag{2}$$

The extra stress tensor $\bar{S}$ and stress tensor $\breve{\tau}$ of Jeffrey model is [25]

$$\breve{\tau} = -pI + \bar{S} \tag{3}$$

$$\bar{S} = \frac{\mu}{1+\lambda_1}\left(\dot{\gamma} + \lambda_2 \ddot{\gamma}\right)$$

Where $\lambda_1, \lambda_2, \mu, \dot{\gamma}$ and $\ddot{\gamma}$ are the constants of Jeffrey fluid, coefficient of fluid viscosity and shear stress and dots over the quantities denotes the derivative with respect to time t. p is the pressure, I is the identity tensor.

2.1. Assumptions

Reynolds number: The gastrointestinal or reproductive tracts essentially have a creeping flow of fluid. The Reynolds number is therefore extremely low (1 for ureter, 10 for gastrointestinal tract). Comparing the momentum equation to the linear viscous forces, the inertia term, which is proportional to the square of velocity, can be neglected.

Wavelength: It should be noticed that the vas deferens radius is extremely small in comparison to the Wavelength. Because the wave number is typically low, this situation can benefit from the long wave length approximation theory [8].

2.2. Governing Equations

The governing equations of non-Newtonian fluid such as continuity, momentum, energy and concentration equations are as follows [10,30]

$$\frac{\partial \hat{U}'}{\partial \hat{X}'}+\frac{\partial \hat{V}'}{\partial \hat{Y}'}=0. \tag{4}$$

$$\rho\left(\frac{\partial \hat{U}'}{\partial \hat{t}'}+\frac{\partial \hat{U}'}{\partial \hat{X}'}\hat{U}'+\hat{V}'\frac{\partial \hat{U}'}{\partial \hat{Y}'}\right)=-\frac{\partial P}{\partial \hat{X}'}+\frac{\partial \bar{S}_{\bar{x}\bar{x}}}{\partial \hat{X}'}+\frac{\partial \bar{S}_{\bar{x}\bar{y}}}{\partial \hat{Y}'}$$
$$-\sigma_0 B_0^2\cos\Omega\left(\cos\Omega\hat{U}'-\sin\Omega\hat{V}'\right)-\frac{\mu}{k_1}\hat{U}'+g\rho\sin\alpha \tag{5}$$

$$\rho\left(\frac{\partial \hat{V}'}{\partial \hat{t}'}+\frac{\partial \hat{V}'}{\partial \hat{X}'}\hat{U}'+\frac{\partial \hat{V}'}{\partial \hat{Y}'}\hat{V}'\right)=-\frac{\partial P}{\partial \hat{Y}'}+\frac{\partial \bar{S}_{\bar{x}y}}{\partial \hat{X}'}+\frac{\partial \bar{S}_{\bar{y}\bar{y}}}{\partial \hat{Y}'}$$
$$-\frac{\mu}{k_1}\hat{V}'+\sigma_0 B_0^2\sin\Omega\left(\cos\Omega\hat{U}'-\sin\Omega\hat{V}'\right)-g\rho\cos\alpha \tag{6}$$

$$\rho c_p\left(\frac{\partial T}{\partial \hat{t}'}+\frac{\partial T}{\partial \hat{X}'}\hat{U}'+\frac{\partial T}{\partial \hat{Y}'}\hat{V}'\right)=\kappa_t\left(\frac{\partial^2 T}{\partial \hat{X}'^2}+\frac{\partial^2 T}{\partial \hat{Y}'^2}\right)+$$
$$\mu\left(\frac{1}{1+\lambda_1}\left(1+\lambda_2\left(\frac{\partial}{\partial \hat{t}'}+\hat{U}'\frac{\partial}{\partial \hat{X}'}+\hat{V}'\frac{\partial}{\partial \hat{Y}'}\right)\right)\left(2\left(\frac{\partial \hat{U}'}{\partial \hat{X}'}\right)^2+2\left(\frac{\partial \hat{V}'}{\partial \hat{Y}'}\right)^2+\left(\frac{\partial \hat{U}'}{\partial \hat{Y}'}+\frac{\partial \hat{V}'}{\partial \hat{X}'}\right)^2\right)\right) \tag{7}$$

$$\frac{\partial C}{\partial \hat{t}'}+\hat{U}'\frac{\partial C}{\partial \hat{X}'}+\hat{V}'\frac{\partial C}{\partial \hat{Y}'}=D_m\left(\frac{\partial^2 C}{\partial \hat{X}'^2}+\frac{\partial^2 C}{\partial \hat{Y}'^2}\right)+\frac{D_m K_T}{T_m}\left(\frac{\partial^2 T}{\partial \hat{X}'^2}+\frac{\partial^2 T}{\partial \hat{Y}'^2}\right)-k_0(C-C_0) \tag{8}$$

Where $\hat{V}',\hat{U}'$ are the velocity on the directions of transverse and axial side, $p,\hat{t}',\rho,\mu,\sigma_0,c_p,k_1,S_{ij},\Omega,\kappa_t$, k_0 represents the pressure, time, density, viscosity, electrical conductivity, specific heat at constant pressure, permeability parameter, extra stress tensor, inclination angle, thermal conductivity, chemical reaction parameter and B_0 is the applied magnetic field.

The extra stress tensor (S_{ij}) of Jeffrey fluid model as follows [14,27, 30]

$$S_{xx}=\frac{2\mu}{1+\lambda_1}\left[1+\lambda_2\left(\frac{\partial}{\partial \hat{t}'}+\hat{U}'\frac{\partial}{\partial \hat{X}'}+\hat{V}'\frac{\partial}{\partial \hat{Y}'}\right)\right]\frac{\partial \hat{U}'}{\partial \hat{X}'} \tag{9}$$

$$S_{xy}=\frac{\mu}{1+\lambda_1}\left[1+\lambda_2\left(\frac{\partial}{\partial \hat{t}'}+\hat{U}'\frac{\partial}{\partial \hat{X}'}+\hat{V}'\frac{\partial}{\partial \hat{Y}'}\right)\right]\left(\frac{\partial \hat{U}'}{\partial \hat{Y}'}+\frac{\partial \hat{V}'}{\partial \hat{X}'}\right) \tag{10}$$

$$S_{yy} = \frac{2\mu}{1+\lambda_1}\left[1+\lambda_2\left(\frac{\partial}{\partial \hat{t}'} + \hat{U}'\frac{\partial}{\partial \hat{X}'} + \hat{V}'\frac{\partial}{\partial \hat{Y}'}\right)\right]\frac{\partial \hat{V}'}{\partial \hat{Y}'} \tag{11}$$

The flow of the fluid is unsteady in the wave frame. So it's convert into steady flow by the following transform (wave frame to fixed frame) [7,12]

$$v' = \hat{V}',\ u' = \hat{U}' - c,\ y' = \hat{Y}'\ x' = \hat{X}' - c\hat{t}' \tag{12}$$

Introducing the dimensionless variables is as follows

$$\begin{aligned} &x = \frac{x'}{\lambda}, u = \frac{u'}{c}, y = \frac{y'}{d_1}, h_1 = \frac{\bar{h}_1}{d_1}, h_2 = \frac{\bar{h}_2}{d_1}, t = \frac{c\bar{t}}{\lambda}, b = \frac{b_1}{d_1}, a = \frac{a_1}{d_1}, d = \frac{d_2}{d_1}, \\ &v = \frac{v'}{c\delta}, S_{ij}^{\ *} = \frac{d_1 S_{ij}}{c\mu}, \theta = \frac{T-T_0}{T_1-T_0}, p = \frac{d_1^2}{\mu\lambda c}\bar{P}, \sigma = \frac{C-C_0}{C_1-C_0} \end{aligned} \tag{13}$$

In which $\mathrm{Re} = \frac{\rho c d_1}{\mu}$ -Reynolds number, a and b are Amplitude of the waves, $\delta = \frac{d_1}{\lambda}$ -Wave number, $E = \frac{c^2}{c_p(T_1 - T_0)}$ -Eckert number, $M = \sqrt{\frac{\sigma_0}{\mu}} B_0 d_1$ -Hartmann number, $\mathrm{Pr} = \frac{\mu c_p}{\kappa_t}$ is the Prandtl number, $Da = \frac{k_1}{d_1^2}$ -Darcy number, $Sr = \frac{\rho D_m (T_1 - T_0) K_T}{\mu T_m (C_1 - C_0)}$ -Soret number, $Br = E\,\mathrm{Pr}$ - Brinkmann number, $Sc = \frac{\mu}{\rho D_m}$ -Schmidt number, $\gamma_1 = \frac{\rho k_0 d_1^2}{\mu}$ -Chemical reaction parameter, $Fr = \frac{c^2}{g d_1}$ -Froude number.

Applying Eqs. (12),(13) into Eqs.(4)-(11), Eq.(4) is fully satisfied. Under the assumptions lubrication theory, Eqs. (5) - (8) becomes

$$\frac{\partial p}{\partial x} = \frac{\partial S_{xy}}{\partial y} - M^2 \cos^2 \Omega (u+1) - \frac{1}{Da}(u+1) + \frac{\mathrm{Re}}{Fr} Sin\alpha\,, \tag{14}$$

$$\frac{\partial p}{\partial y} = 0\,, \tag{15}$$

$$\frac{1}{\mathrm{Pr}}\frac{\partial^2 \theta}{\partial y^2} + \frac{E}{1+\lambda_1}\left(\frac{\partial u}{\partial y}\right)^2 = 0 \tag{16}$$

$$\frac{1}{Sc}\frac{\partial^2 \sigma}{\partial y^2} + Sr\frac{\partial^2 \theta}{\partial y^2} - \gamma_1 \sigma = 0 \tag{17}$$

The stream functions are

$$v = -\delta\frac{\partial \psi}{\partial x}, u = \frac{\partial \psi}{\partial y} \tag{18}$$

Eqs. (14) and (16) in terms of stream function ψ can be rewritten by

$$\frac{\partial p}{\partial x}=\frac{1}{1+\lambda_1}\frac{\partial^3\psi}{\partial y^3}-\left(M^2\cos^2\Omega+\frac{1}{Da}\right)\left(\frac{\partial\psi}{\partial y}+1\right)+\frac{\mathrm{Re}}{Fr}\sin\alpha \tag{19}$$

$$\frac{\partial^2\theta}{\partial y^2}+\frac{Br}{1+\lambda_1}\left(\frac{\partial^2\psi}{\partial y^2}\right)^2=0 \tag{20}$$

$$\frac{\partial^2\sigma}{\partial y^2}+ScSr\frac{\partial^2\theta}{\partial y^2}-Sc\gamma_1\sigma=0 \tag{21}$$

From Eq.(15),we conclude that pressure is independent on y. Now, eliminating pressure gradient in Eq.(19) differentiate partially with respect to y we get

$$\frac{\partial^4\psi}{\partial y^4}-A_1^2\frac{\partial^2\psi}{\partial y^2}=0, \tag{22}$$

The corresponding boundary conditions of slip conditions are [30]

$$\psi=-\frac{F}{2}\ \text{and}\ \frac{\partial\psi}{\partial y}=\frac{\overline{\eta}_1}{(1+\lambda_1)}\frac{\partial^2\psi}{\partial y^2}+\frac{\overline{\eta}_2}{(1+\lambda_1)}\frac{\partial^3\psi}{\partial y^3}-1\ \text{at}\ y=h_1[=-b\cos(2\pi x+\phi)-d]$$

$$\psi=\frac{F}{2}\ \text{and}\ \frac{\partial\psi}{\partial y}=-\frac{\overline{\eta}_1}{(1+\lambda_1)}\frac{\partial^2\psi}{\partial y^2}-\frac{\overline{\eta}_2}{(1+\lambda_1)}\frac{\partial^3\psi}{\partial y^3}-1\ \text{at}\ y=h_2[=a\cos(2\pi x)+1], \tag{23}$$

$$\theta+\beta\frac{\partial\theta}{\partial y}=0\ \text{at}\ y=h_1\ \text{and}\ \theta-\beta\frac{\partial\theta}{\partial y}=1\ \text{at}\ y=h_2 \tag{24}$$

$$\sigma+\gamma\frac{\partial\sigma}{\partial y}=0\ \text{at}\ y=h_1\ \text{and}\ \sigma-\gamma\frac{\partial\sigma}{\partial y}=1\ \text{at}\ y=h_2 \tag{25}$$

Where F is the flux, $\overline{\eta}_1,\overline{\eta}_2,\beta$ and γ represents first order, second order, thermal, concentration slip parameters respectively and b,a,d and ϕ satisfies the condition

$$b^2+a^2+2ba\cos\phi\le(1+d)^2$$

3. SOLUTION OF THE PRESENT FLOW PATTERN

The exact result of Eqs. (20) - (22) with the help of Eqs. (23) -(25) we get,

$$\psi=c_1+c_2y+c_3\cosh A_1y+c_4\sin A_1y, \tag{26}$$

$$\theta=c_5+c_6y+\frac{A_{14}e^{2A_1y}}{4A_1^2}+\frac{A_{15}e^{-2A_1y}}{4A_1^2}+A_{16}\frac{y^2}{2} \tag{27}$$

$$\sigma=c_7\cosh(\sqrt{Sc\gamma_1}y)+c_8\sinh(\sqrt{Sc\gamma_1}y)-ScSr\left(\frac{A_{14}e^{2A_1y}+A_{15}e^{-2A_1y}}{4A_1^2-Sc\gamma_1}-\frac{A_{16}}{Sc\gamma_1}\right) \tag{28}$$

Where $c_i, i=1-8$, are constants which are presented in the appendix.

Substitute Eq. (26) into Eq. (19) and get the pressure gradient in the axial direction is

$$\frac{\partial p}{\partial x}=\frac{1}{1+\lambda_1}A_1^3c_4-A_1^2\left(c_2+A_1c_4+1\right)+\frac{\mathrm{Re}}{Fr}\sin\alpha\,, \tag{29}$$

Pressure rise is calculated numerically per wave length by the following formula

$$\Delta p_\lambda=\int_0^{2\pi}\frac{dp}{dx}dx \tag{30}$$

The possible wave shapes namely Sawtooth, Trapezoidal, Triangular and Square wave forms are modeled from the Fourier series as follows [8]

Sawtooth waveform:

$$h_1=1+a\frac{8}{\pi^3}\sum_{j=1}^{\infty}\frac{\sin(2j\pi x)}{j},\ h_2=-d-b\frac{8}{\pi^3}\sum_{j=1}^{\infty}\frac{\sin\left[(2j\pi x)+\phi\right]}{j}$$

Trapezoidal waveform:

$$h_1=1+a\frac{32}{\pi^2}\sum_{j=1}^{\infty}\frac{\sin\frac{\pi}{8}(2j-1)}{(2j-1)^2}\sin[2\pi(2j-1)x],$$

$$h_2=-d-b\frac{32}{\pi^2}\sum_{j=1}^{\infty}\frac{\sin\frac{\pi}{8}(2j-1)}{(2j-1)^2}\sin[2\pi(2j-1)x+\phi]$$

Triangular waveform:

$$h_1=1+a\frac{8}{\pi^3}\sum_{j=1}^{\infty}\frac{(-1)^{j+1}\sin[2\pi(2j-1)x]}{(2j-1)^2},\ h_2=-d-b\frac{8}{\pi^3}\sum_{j=1}^{\infty}\frac{(-1)^{j+1}\sin[2\pi(2j-1)x+\phi]}{(2j-1)^2}$$

Square waveform:

$$h_1=1+a\frac{4}{\pi}\sum_{j=1}^{\infty}\frac{(-1)^{j+1}\cos[2\pi(2j-1)x]}{(2l-1)},\ h_2=-d-b\frac{4}{\pi}\sum_{j=1}^{\infty}\frac{(-1)^{j+1}\cos[2\pi(2j-1)x+\phi]}{(2j-1)}$$

4. Result and Discussion

The graphical result of velocity, pressure rise, pressure gradient, temperature and concentration profiles are plotted by the computational mathematical software Matlab and the streamlines are drawn by Mathematica.

4.1. Velocity Profile

Figs.2(a-d) presented for variation of the velocity profile (u) for changing the values of M (Hartmann number), Da (Darcy number), λ_1 (Jeffrey fluid parameter) and ϕ (phase difference). Fig. 2(a) shows that, for larger values of Hartmann number M velocity of the fluid diminishes in the core part of the (porous) channel also quit opposite behavior concluded

near the boundary of the channel walls. That means larger magnetic field decline the fluid velocity in the axial direction as Lorentz force plays retarding force in the fluid movement [32, 33]. Fig.2(b). illustrates the impact of Darcy number Da on the velocity profile. This figure seems, increase Da means diminish the drag force and that cause enhance the axial velocity. Fig.2(c) plotted for impact of Jeffrey fluid parameter λ_1. From this figure we concluded that the axial velocity diminishes for greater λ_1. Also observe that, In the case of Newtonian fluid (λ_1=0) the velocity is maximum. The fluid velocity reduces near the left wall of the channel when the phase angle ϕ increases is presented in Fig. 2(d).

4.2. Pressure rise and pressure gradient

The pumping characteristics against the dimensionless flow rate for changing the values of Hartmann number M ,Darcy number Da , Jeffrey fluid parameter λ_1 and Frude number Fr are presented in Figs.3(a-d). Pressure rise enhances in retrograde region $(\Theta < 0, \Delta p_\lambda > 0)$ and decrease in co-pumping region $(\Theta > 0, \Delta p_\lambda < 0)$ for increasing of Hartmann number and λ_1. But in the peristaltic pumping region $(\Theta > 0, \Delta p_\lambda > 0)$ pressure rise increases up to $\Theta \in [0,0.1]$ and diminished for $\Theta > 0.1$ but opposite behavior is concluded for large values of Da (Darcy number). Pressure rise decrease throughout the region (Retrograde region, pumping region and co-pumping region) for the values of Frude number Fr enhances. Pressure gradient for different values of M , Jeffrey fluid parameter λ_1 and Frude number Fr are illustrated through the Figs. 4(a-c). Pressure gradient $\frac{dp}{dx}$ raises throughout the channel when large values of M and Frude number see Figs.4(a,c). Pressure gradient against the Jeffrey fluid parameter λ_1 is presented in Fig.4(b). From this figure we observe that, the pressure rise diminishes when $x \in [0.6,0.8]$ and enhances rest of the region.

4.3. Heat and Mass transfer

Variations of temperature distribution for Hartmann number M, Darcy number Da, Jeffrey fluid parameter λ_1, slip parameter β and Brinkmann number Br are illustrated in Figs 5(a-e). For greater values of M (Hartmann number), the temperature of the fluid enhances see Fig.5(a). This figure shows that the temperature of the magnetohydrodynamic fluid is larger when compare to hydrodynamic fluid. The energy dissipation leads to increase the fluid temperature gets compensated by the presence of porous medium is work done with

internal resistance. Since the fluid temperature is diminished larger values of Da. Temperature of the fluid enhances for λ_1 and Br increases see Figs.5(c,e). Temperature of the fluid decreases when the value of slip parameter β enhances see Fig.2(d).

Fig.6(a,b) was developed to demonstrate how the amplitude (a) and parameter of a chemical reaction (γ_1) affect the concentration profile. The concentration of the fluid decreases when chemical reaction parameter (γ_1) and amplitude (a) are enhanced. Chemical reaction boosts the rate of mass transfer across interfaces, which reduces concentration. The concentration decreases as you increase in Schmidt number (Sc), as shown in Fig. 6(c). Schmidt number is used to characterize fluid flows in which there are simultaneous momentum and mass diffusion convection processes. The density of the fluid particles reduces as the Schmidt number (Sc) rises in value. It helps the particles go away more faster, thus reduces concentration. For rising values of the Soret number (Sr), a decrease in concentration is seen; see Fig. 6(d).

4.4. Trapping phenomenon

Trapping is an important mechanism for analyzing the peristaltic fluid flow pattern. Streamlines for different values of M and λ_1 is displayed in Figs. 7 and 8. Fig.7 depicts that the size of trapped bolus diminishes in the lower wall for enhancing the Hartmann number (M). In the both walls of the channel trapped bolus size decreases for large values of λ_1. Finally, the trapped bolus disappears in the both walls for increasing the values of Jeffrey fluid parameter λ_1 see Fig.8. Different wave forms of the streamlines such as sawtooth wave, square wave, trapezoidal wave, triangular wave are presented in Fig.9. Present study is validated with previous study of Misra and Rao [31] with $(M = 0, Da \to \infty, \alpha = 0)$. From this figure we conclude that, present study is accordance with existing literature see Fig.10.

5. Conclusion

In this study, we investigated the influence of velocity slip conditions on the peristaltic motion of the Jeffrey fluid in the asymmetric channel with porous medium, magnetic field and chemical reactions. The governing equations are reduced long wavelength and the small Reynolds number approximations. The resulting governing equations are solved by the exact solution. The key findings are as follows

1 The axial velocity decreases for enhancing M, λ_1 and ϕ but the opposite trend concluded for increasing Da.

2 The pressure rise raises in the pumping region for greater values of M, λ_1 and decreases for Da.

3 Pressure rise decreases throughout the region for increasing Fr.

4 The temperature raises when enhancing M, λ_1 and Br but opposite trend concluded for increasing Da and β.

5 The concentration of the fluid diminished for enhancing γ_1, a, Sc and Sr.

6 The size of the trapped bolus diminishes for larger values of M and λ_1.

References

[1] Latham, T.W. "Fluid motion in a peristaltic pump", *MS Thesis*. Cambridge M.A: MIT (1966).

[2] Brown,T.D. and Hung, T.K. "Computational and experimental investigation of two-dimensional nonlinear peristaltic flow", *J. Fluid Mech.*, **83,** pp. 249–273 (1977).

[3] Vajravelu, K. Sreenadh, S. and Babu, V.R. "Peristaltic transport of Herschel-Bulkley fluid in an inclined tube", *J. Nonlinear Mech.*, **40,**pp. 83–90, (2005).

[4] Wang, Y. Hayat, T. and Hutter, K. "Peristaltic flow of a Johnson Segalman fluid through a deformable tube", *Theor Comput Fluid Dyn.*, **21**, pp.369–380, (2007).

[5] Bhatti, M.M. Abdelsalam, S.I. "Bio-inspired peristaltic propulsion of hybrid nanofluid flow with Tantalum (Ta) and Gold (Au) nanoparticles under magnetic effects", *Waves in Random and Complex Media.*, DOI: 10.1080/17455030.2021.1998728 (2021).

[6] Magesh, A. Kothandapani, M. and Pushparaj,V. "Electro-Osmotic flow of Jeffry fluid in an asymmetric micro channel under the effect of magnetic field", *J Phys: Conf Ser.*, **1850:** 012102, (2021).

[7] Magesh, A. Tamizharasi, P. and Vijayaragavan, R. "MHD flow of (Al_2O_3/H_2O) nanofluid under the peristaltic mechanism in an asymmetric channel", *Heat Transf.*, vol.**51(7)**, pp. 6563-6577,(2022).

[8] Magesh, A, Tamizharasi, P. and Kamalakkannan, "Analysis of Bejan number and Entropy generation of Non-Newtonian nanofluid through an asymmetric microchannel", *Numer Heat Transf part A: Appl.* Doi: 10.1080/10407782.2023.2240507 (2023).

[9] Muthuraj, R. Nirmala, K. and Srinivas, S. “Influences of chemical reaction and wall properties on MHD Peristaltic transport of a Dusty fluid with Heat and Mass transfer”, *Alexandr Eng J.*, **55,** pp.597–611,(2016).

[10] Magesh, A. Praveen Kumar, P. Tamizharasi, et al., “Effect of magnetic field on the peristaltic transport of Oldroyd-B fluid in an asymmetric inclined channel”, *J Phys: Conf Ser*.,1850: 012111, (2021).

[11] Tamizharasi, P. Vijayaragavan, R. and Magesh, A. “Electro-osmotic driven flow of Eyring Powell nanofluid in an asymmetric channel”, *Math Methods Appl Sci.*, pp.1–18. DOI 10.1002/mma.9270, (2023).

[12] Tamizharasi, P. Vijayaragavan, R. and Magesh, A. “Heat and Mass transfer analysis of the peristaltic driven flow of nanofluid in an asymmetric channel”, *Partial Diff Equ Appl Math*.**, 4:** 100087, (2021).

[13] Magesh, A. Kothandapani, M. “Analysis of heat and mass transfer on the peristaltic movement of Carreau nanofluids”, *J Mech Med Biol.,* **21(9):** 2150068, (2021).

[14] Rabeeah, R. Rahila, N. and Sara I. Abdelsalam. “Microorganisms swimming through radiative Sutterby nanofluid over stretchable cylinder: Hydrodynamic effect”, *Numer. Methods Partial Differential Equations.*,39(2), pp.975-994, (2023).

[15] Darcy, H. Les fontaines publiques de la ville de Dijon. Paris: Dalmont; 1856.

[16] Mekheimer, Kh.S. “Non-linear peristaltic transport through a porous medium in an inclined planner channel”, *J Por Media,* **6,** pp.189–201,(2003).

[17] Sheikholeslami, M., Hatami, M. and Ganji, D.D. “Analytical investigation of MHD nanofluid flow in a semi-porous channel”, *Powder Technol*, **246,** pp. 327-336, (2013).

[18] Patil, P.M. and Chamkha, A. “Heat and mass transfer from mixed convection flow of polar fluid along a plate in porous media with chemical reaction”, *Int. J. Numer Methods Heat Fluid Flow,* **23**, pp.899-926, (2013).

[19] Gnaneswara Reddy, M. and Venugopal Reddy, K. “Impact of velocity slip and joule heating on MHD peristaltic flow through a porous medium with chemical reaction”, *J. Niger Mathematical Society,* **35**, pp. 227–244,(2016).

[20] Eldesoky, I.M., Abdelsalam, S.I., Wageeh A. El-Askary., et al. “The integrated thermal effect in conjunction with slip conditions on peristaltically induced particle-fluid transport in a catheterized pipe”, *J. Por. Media,* pp. 695-713, (2020). Doi: 10.1615/JPorMedia.2020025581.

[21] Khan, Z.H. Makinde, O.D. Hamid, M. et al.“Hydromagnetic flow of ferrofluid in an enclosed partially heated trapezoidal cavity filled with a porous medium”, *J. Magn.Magn. Mater*.**499**, pp. 166241, (2020)

[22] Kamalakkannan, J. Dhanapal, C. Kothandapani, M. and Magesh, A. (2023), "Peristaltic transport of non-Newtonian nanofluid through an asymmetric microchannel with electroosmosis and thermal radiation effects", *Indian J Phys.* DOI:10.1007/s12648-023-02636-9.

[23] Sara I Abdelsalam, Magesh, A, Tamizharasi, P and Zaher, AZ." Versatile response of a Sutterby nanofluid under activation energy through an asymmetric conduit: Hyperthermia therapy", *Int. J. Numer. Methods Heat Fluid Flow,* DOI 10.1108/HFF-04-2023-0173 (2023).

[24] Vijayaragavan, R. Tamizharasi, P. and Magesh, A. "Brownian motion and thermoporesis effects of nanofluid flow through the peristaltic mechanism in a vertical channel", *J Por Media.,**25(6)**,* pp.65-81, (2022).

[25] Bhatti, M.M. Arain, M.B. Zeeshan, A. et al."Swimming of Gyrotactic Microorganism in MHD Williamson nanofluid flow between rotating circular plates embedded in porous medium: Application of thermal energy storage", *J. Energy Storage,***45,** pp. 103511, (2022).

[26] Nadeem, S. Riaz, A. Ellahi, R. et al. "Mathematical model for the peristaltic flow of Jeffrey fluid with nanoparticles phenomenon through a rectangular duct", *Appl. Nanosci.,* DOI 10.1007/s13204-013-0238-5.

[27] Bhatti, M.M. Zeeshan, A. and Ellahi, R. "Simultaneous effects of coagulation and variable magnetic field on peristaltically induced motion of Jeffrey nanofluid containing gyrotactic microorganism", *Microvasc Research,* **110**, pp.32–42,(2017).

[28] Bhatti, M.M. Alamri, S.Z. Ellahi, R. et al. "Intra-uterine particle–fluid motion through a compliant asymmetric tapered channel with heat transfer", *J.Therm. Anal. Calorim.,* **144**, pp. 2259–2267, (2021).

[29] Magesh, A. and Kothandapani, M. "Heat and mass transfer analysis on non-Newtonian fluid motion driven by peristaltic pumping in an asymmetric curved channel", *Eur. Phys. J. Spec. Top.,* **230**, pp.1447-1464, (2021).

[30] Saleem, N. Akram, S. Afzal, F. et al. "Impact of velocity second slip and inclined magnetic field on peristaltic flow coating with Jeffrey fluid in tapered channel", *Coatings,* **10, pp.**30,(2020).

[31] Mishra, M. and Rao, A.R. "Peristaltic transport of a Newtonian fluid in an asymmetric channel", *Z. Angew Math Phys.* **54**, pp. 532-550, (2003).

[32] Abd Elmaboud, Y. and Abdelsalam, S.I. "DC/AC magnetohydrodynamic-micropump of a generalized Burger's fluid in an annulus", *Phys Scr.,* **94**, pp. 115209, (2019).

[33] Bhatti, M.M. and Abdelsalam, S.I. "Thermodynamic entropy of a magnetized Ree-Eyring particle-fluid motion with irreversibility process: A mathematical paradigm", *J Appl Math Mech.*, **101(6)**, pp. 1-17, (2021).

Appendix

$$A_1^2 = (1+\lambda_1)\left[M^2\cos^2\theta + \frac{1}{Da}\right],\ A_2 = A_1\sinh A_1h_1 + \frac{\eta_1}{(1+\lambda_1)}A_1^2\cosh A_1h_1 + \frac{\eta_2}{(1+\lambda_1)}A_1^3\sinh A_1h_1,$$

$$A_3 = A_1\cosh A_1h_1 + \frac{1}{(1+\lambda_1)}\left[\eta_1A_1^2\sinh A_1h_1 + \eta_2A_1^3\cosh A_1h_1\right],$$

$$A_4 = A_1\sinh A_1h_2 - \frac{1}{(1+\lambda_1)}\left[\eta_1A_1^2\cosh A_1h_2 + \eta_2A_1^3\sinh A_1h_2\right],$$

$$A_5 = A_1\cosh A_1h_2 - \frac{1}{(1+\lambda_1)}\left[\eta_1A_1^2\sinh A_1h_2 + \eta_2A_1^3\cosh A_1h_2\right],$$

$$A_6 = h_2 - h_1,\ A_7 = \cosh A_1h_2 - \cosh A_1h_1,\ A_8 = \sinh A_1h_2 - \sinh A_1h_1,\ A_9 = A_4 - A_2,\ A_{10} = A_5 - A_3,$$

$$A_{11} = A_7 - A_4A_6,\ A_{12} = A_8 - A_5A_6,\ c_4 = \frac{(F + A_6)A_9}{A_{12}A_9 - A_{10}A_{11}},\ c_3 = -c_4\frac{A_{10}}{A_9}$$

$$c_2 = -1 - c_3A_4 - c_4A_5,\ c_1 = \frac{F}{2} - c_2h_2 - c_3\cosh A_1h_2 - c_3\sinh A_1h_2$$

$$A_{14} = -A_{13}\left(\frac{c_3^2}{4} + \frac{c_4^2}{4} + \frac{c_3c_4}{2}\right),\ A_{15} = -A_{13}\left(\frac{c_3^2}{4} + \frac{c_4^2}{4} - \frac{c_3c_4}{2}\right),\ A_{16} = -2A_{13}\left(\frac{c_3^2}{4} - \frac{c_4^2}{4}\right),$$

$$A_{17} = \frac{A_{14}e^{2A_1h_1}}{4A_1^2} + \frac{A_{15}e^{-2A_1h_1}}{4A_1^2} + \frac{A_{16}h_1^2}{2} + \beta\left[\frac{A_{14}e^{2A_1h_1}}{2A_1} - \frac{A_{15}e^{-2A_1h_1}}{2A_1} + A_{16}h_1\right]$$

$$A_{18} = \frac{A_{14}e^{2A_1h_2}}{4A_1^2} + \frac{A_{15}e^{-2A_1h_2}}{4A_1^2} + \frac{A_{16}h_2^2}{2} - \beta\left[\frac{A_{14}e^{2A_1h_2}}{2A_1} - \frac{A_{15}e^{-2A_1h_2}}{2A_1} + A_{16}h_2\right]$$

$$c_6 = \frac{1 + A_{17} - A_{18}}{A_6 - 2\beta},\ c_5 = -(A_{17} + c_6(h_1 + \beta)),\ l_1 = \cosh\left(\sqrt{Sc\gamma_1}h_1\right) + \gamma\sqrt{Sc\gamma_1}\sinh\left(\sqrt{Sc\gamma_1}h_1\right),$$

$$l_2 = \sinh\left(\sqrt{Sc\gamma_1}h_1\right) + \gamma\sqrt{Sc\gamma_1}\cosh\left(\sqrt{Sc\gamma_1}h_1\right),$$

$$l_3 = -ScSr\left(\frac{A_{14}e^{2A_1h_1}(1+2A_1\gamma) + A_{15}e^{-2A_1h_1}(1-2A_1\gamma)}{4A_1^2 - Sc\gamma_1} - \frac{A_{16}}{Sc\gamma_1}\right),$$

$$l_4 = \cosh\left(\sqrt{Sc\gamma_1}h_2\right) + \gamma\sqrt{Sc\gamma_1}\sinh\left(\sqrt{Sc\gamma_1}h_2\right),\ l_5 = \sinh\left(\sqrt{Sc\gamma_1}h_2\right) + \gamma\sqrt{Sc\gamma_1}\cosh\left(\sqrt{Sc\gamma_1}h_2\right),$$

$$l_6 = -ScSr\left(\frac{A_{14}e^{2A_1h_2}(1+2A_1\gamma) + A_{15}e^{-2A_1h_2}(1-2A_1\gamma)}{4A_1^2 - Sc\gamma_1} - \frac{A_{16}}{Sc\gamma_1}\right),\quad c_7 = -(l_2c_8 + l_3)/l_1,$$

$$c_8 = \frac{l_3l_4 + l_1 - l_1l_6}{l_1l_5 - l_2l_4}$$

List of figure captions

Figure 1. Physical model of the channel

Figure 2. Velocity distribution for $(a)\phi = \frac{\pi}{6}, \lambda_1 = 0.2, Da = 0.4,$ $(b)\phi = \frac{\pi}{6}, \lambda_1 = 0.2, M = 0.2,$

$(c)\phi = \frac{\pi}{6}, Da = 2, M = 0.5,$ $(d)Da = 2, \lambda_1 = 0.5, M = 0.5,$ and other values are

$d = 1.1, a = 0.6, x = 0.1, b = 0.5, \overline{\eta}_1 = 0.002, \overline{\eta}_2 = 0.003, \Theta = 1.9, l = \frac{\pi}{4}$

Figure 3. Variation of pressure rise $(a)\lambda_1 = 0.7, Da = 0.2, Fr = 0.6,$

$(b)\lambda_1 = 0.7, Fr = 0.6, M = 1.5,$ $(c)Da = 1, Fr = 0.6, M = 1.5,$ $(d)Da = 0.2, \lambda_1 = 0.7, M = 2$ and

other values are $d = 1.1, a = 0.4, b = 0.3, \phi = \frac{\pi}{6}, \overline{\eta}_1 = 0.4, \overline{\eta}_2 = 0.5, , l = \frac{\pi}{6}, \mathrm{Re} = 0.4, \alpha = 0.2$

Figure 4. Variation of pressure gradient

$(a)Fr = 0.5, \lambda_1 = 0.7,$ $(b)Fr = 0.6, M = 1.5$ $(c)M = 1.5, Fr = 0.6$ and other values are

$d = 1.1, a = 0.4, b = 0.3, \phi = \frac{\pi}{6}, \overline{\eta}_1 = 0.4, \overline{\eta}_2 = 0.5, \alpha = 0.2, l = \frac{\pi}{6}, Da = 0.2, \mathrm{Re} = 0.3,$

Figure 5. Temperature distribution for $(a)\lambda_1 = 0.3, Da = 0.2, \beta = Br = 0.1$

$(b)\lambda_1 = 0.3, M = 2, \beta = Br = 0.1$ $(c)Da = 0.7, M = 1.5, \beta = Br = 0.1$

$(d)Da = 0.2, M = 2, \lambda_1 = 0.5, Br = 0.1$ $(e)M = 2, Da = .\lambda_1 = 0.5, \beta = 0.01$ and other values are

$d = 1.1, a = 0.4, x = 0.1, b = 0.5, \phi = \frac{\pi}{6}, \overline{\eta}_1 = 0.01, \overline{\eta}_2 = 0.02, \Theta = 1.9, l = \frac{\pi}{4}$

Figure 6. Concentration distribution for $(a)a = 0.4, Sr = 0.5, Sc = 1, \gamma = 0.1,$

$(b)Sc = 1, Sr = 0.5, \gamma = 0.1, \gamma_1 = 1$ $(c)a = 0.4, Sr = 0.5, \gamma = 0.1, \gamma_1 = 1$

$(d)a = 0.4, Sc = 1, \gamma = 0.1, \gamma_1 = 1$ and other values are $d = 1.1, b = 0.5, \phi = \frac{\pi}{6}, x = 0.1, \overline{\eta}_1 = 0.01,$

$\overline{\eta}_2 = 0.02, \Theta = 1.9, \lambda_1 = 3, l = \frac{\pi}{4}, M = 2, Da = 0.2, \beta = 0.01, Br = 0.5.$

Figure 7. Streamlines for $(a)M=0(b)M=1(c)M=2(d)M=3$ other values are

$$d=1.1, a=0.4, b=0.5, \phi=\frac{\pi}{12}, x=0.1, \overline{\eta}_1=0.01, \overline{\eta}_2=0.02, \Theta=1.9, \lambda_1=0.2, l=\frac{\pi}{4}, Da=0.3$$

Figure 8. Streamlines for $(a)\lambda_1=0$, $(b)\lambda_1=1$, $(c)\lambda_1=2$ and $(d)\lambda_1=3$ other values are

$$d=1.1, a=0.4, b=0.3, \phi=\frac{\pi}{18}, x=0.1, \overline{\eta}_1=0.01, \overline{\eta}_2=0.02, \Theta=1.9, M=1.5, l=\frac{\pi}{6}, Da=0.2$$

Figure 9. Streamlines for (a) Sawtooth waveform,(b) Square waveform,(c)Triangular waveform,(d) Trapezoidal waveform.

Figure 10. Validation with Misra and Rao [31].

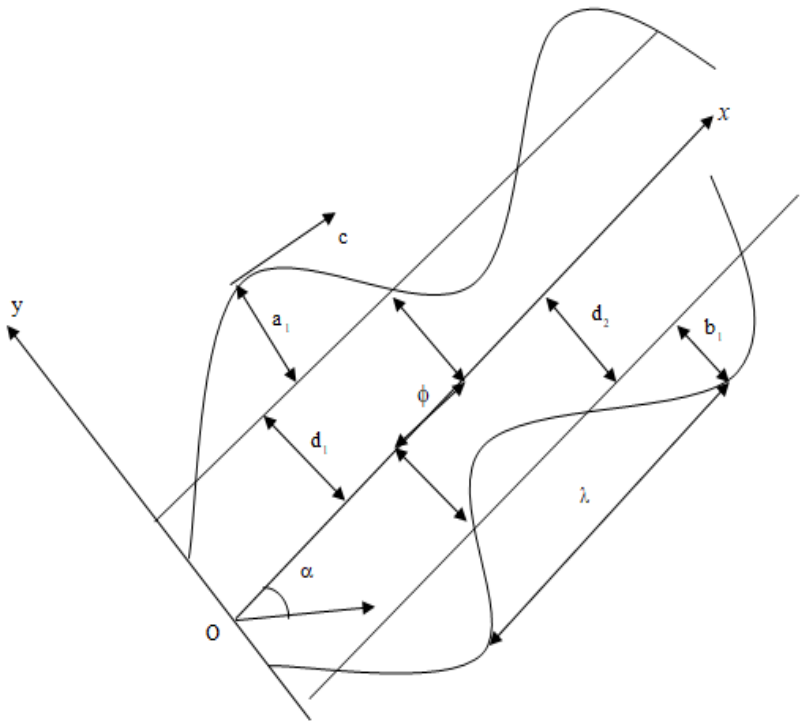

Figure 1.

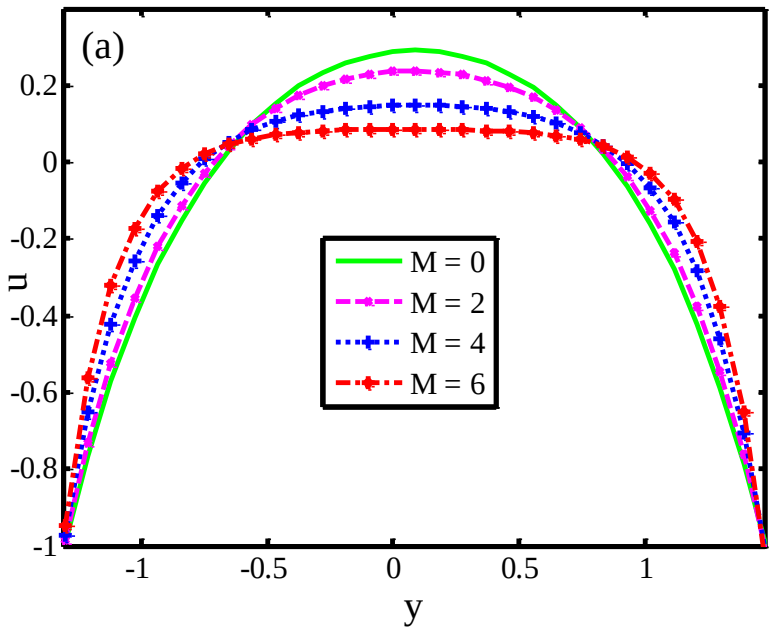
(a)
0.2
0
-0.2
-0.4
-0.6
-0.8
-1
u
-1
-0.5
0
0.5
1
y
M = 0
M = 2
M = 4
M = 6

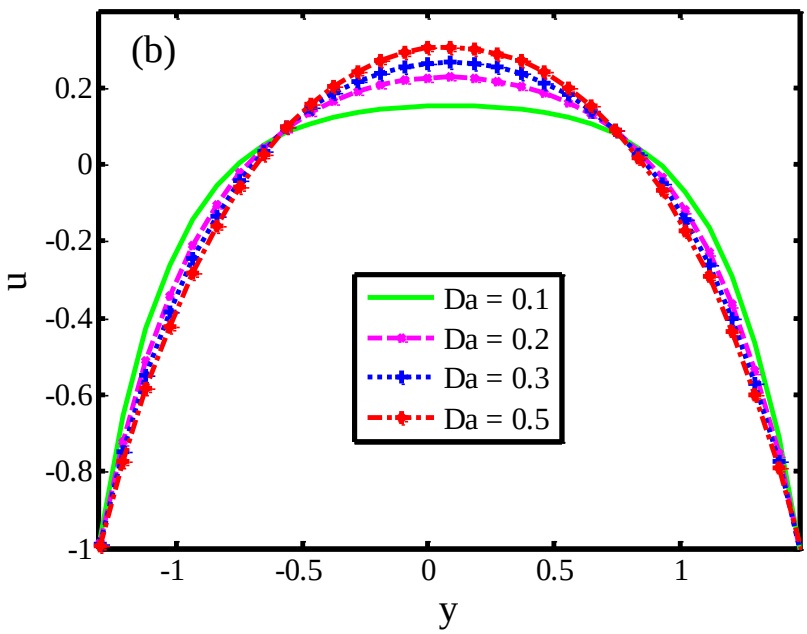
(b)
0.2
0
-0.2
-0.4
-0.6
-0.8
-1
u
-1
-0.5
0
0.5
1
y
Da = 0.1
Da = 0.2
Da = 0.3
Da = 0.5

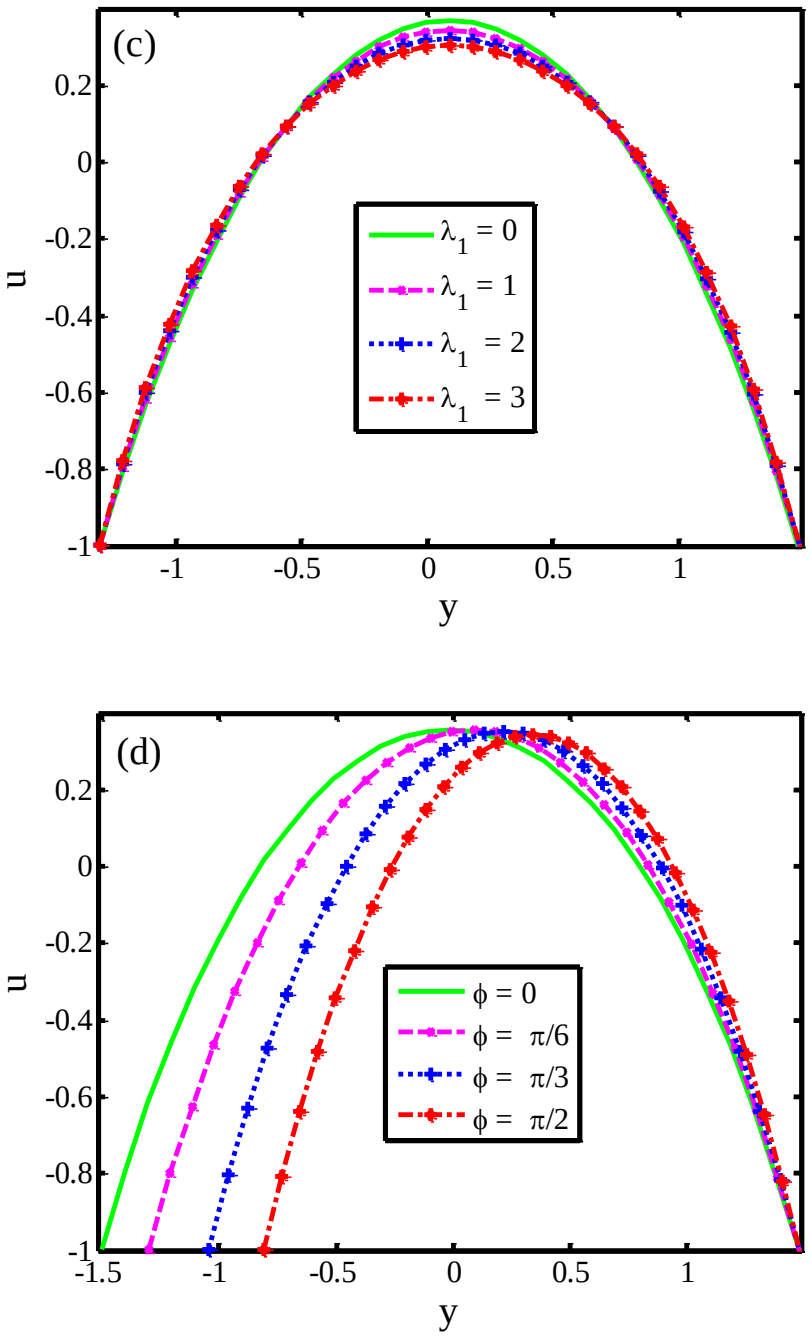
(c)
0.2
0
-0.2
-0.4
-0.6
-0.8
-1
u
-1
-0.5
0
0.5
1
y
λ1 = 0
λ1 = 1
λ1 = 2
λ1 = 3
(d)
0.2
0
-0.2
-0.4
-0.6
-0.8
-1
u
-1.5
-1
-0.5
0
0.5
1
y
ϕ = 0
ϕ = π/6
ϕ = π/3
ϕ = π/2

Figure 2

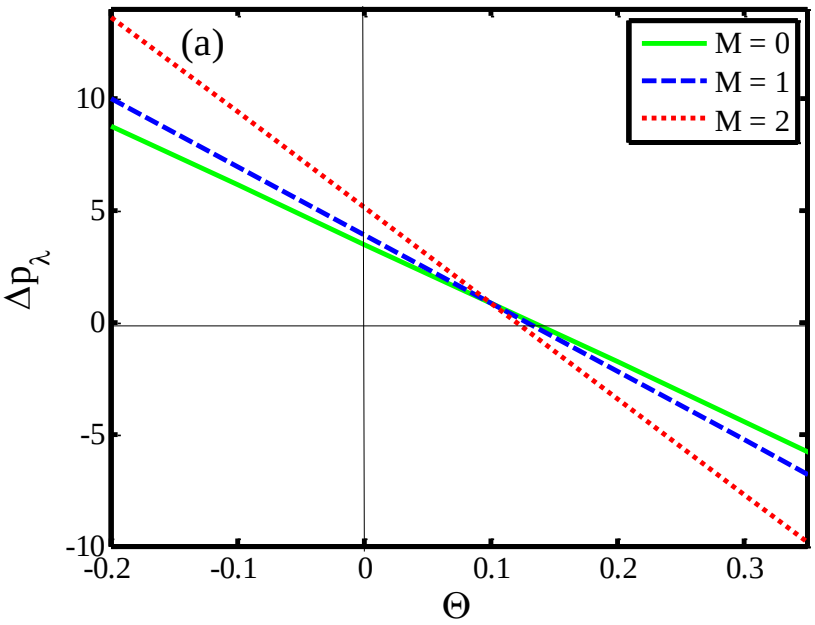
(a)
M = 0
M = 1
M = 2
10
5
0
-5
-10
-0.2
-0.1
0
0.1
0.2
0.3
Δp_λ
Θ

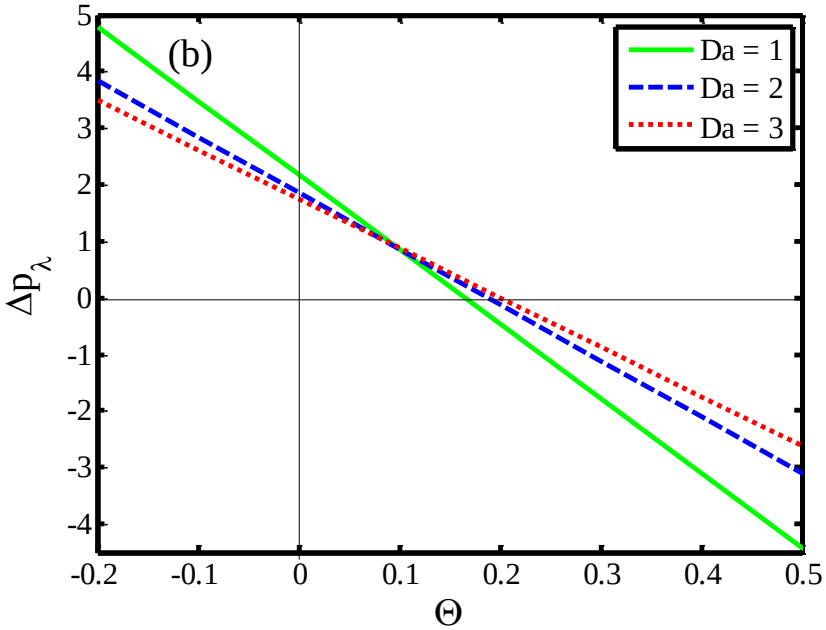
(b)
Da = 1
Da = 2
Da = 3
5
4
3
2
1
0
-1
-2
-3
-4
-0.2
-0.1
0
0.1
0.2
0.3
0.4
0.5
Δp_λ
Θ

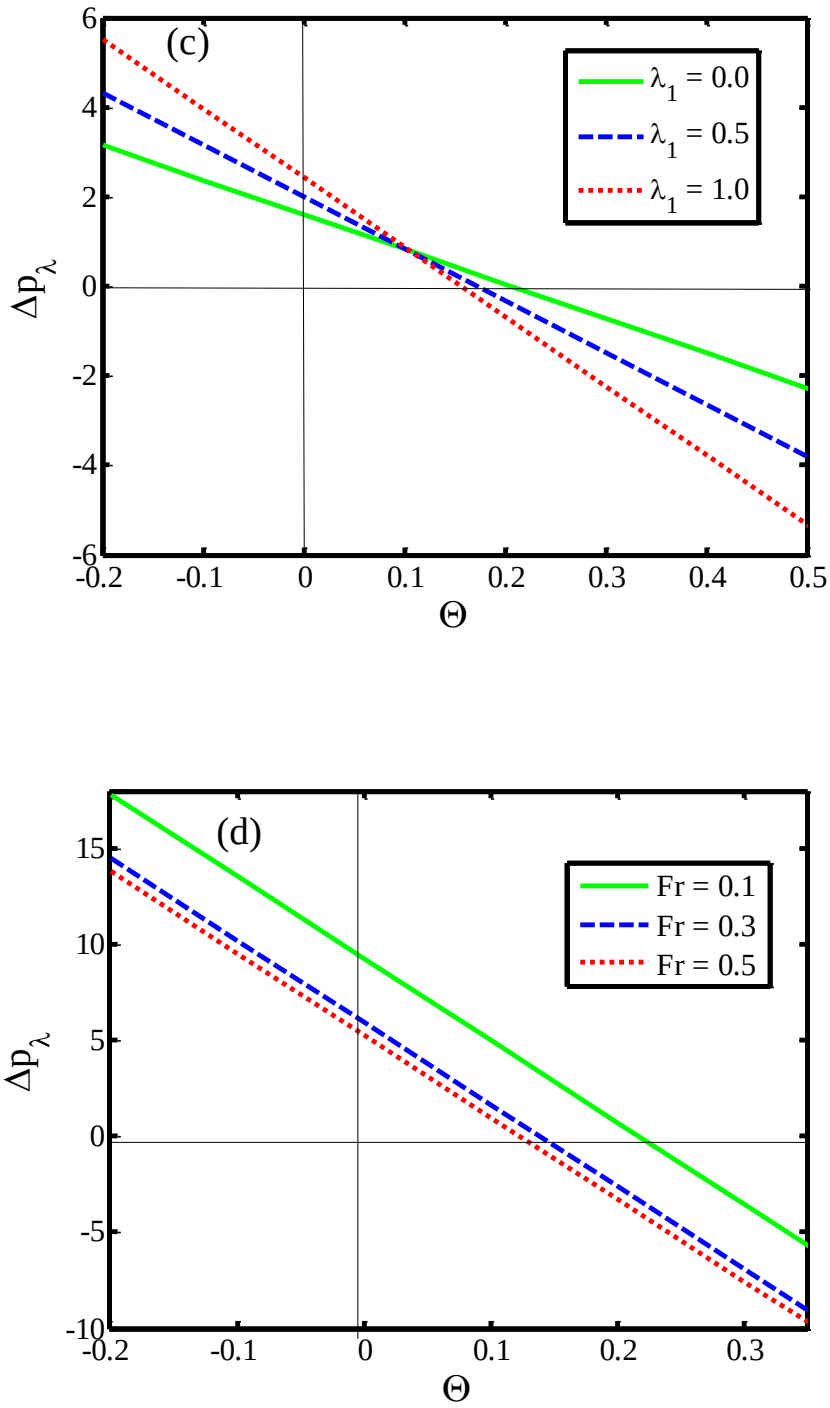

Figure 3.

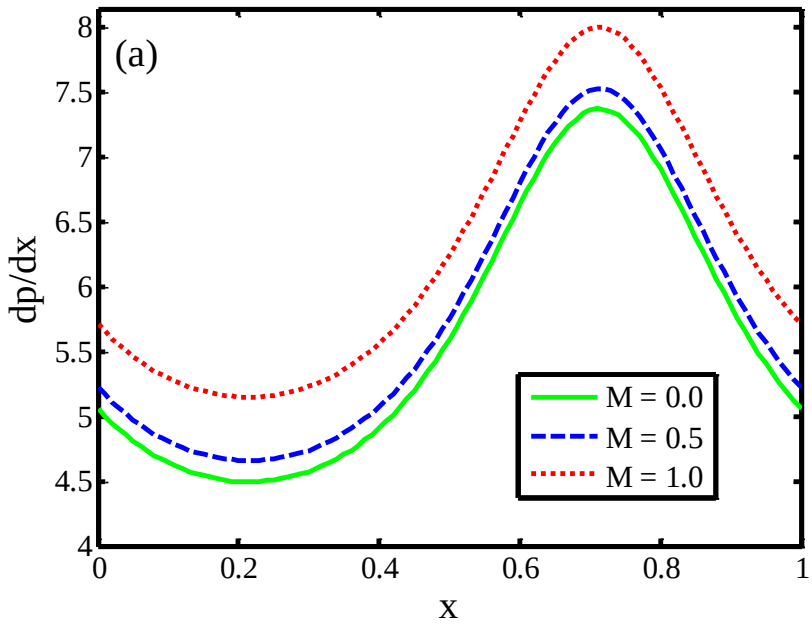
(a)
dp/dx
x
M = 0.0
M = 0.5
M = 1.0
8
7.5
7
6.5
6
5.5
5
4.5
4
0
0.2
0.4
0.6
0.8
1

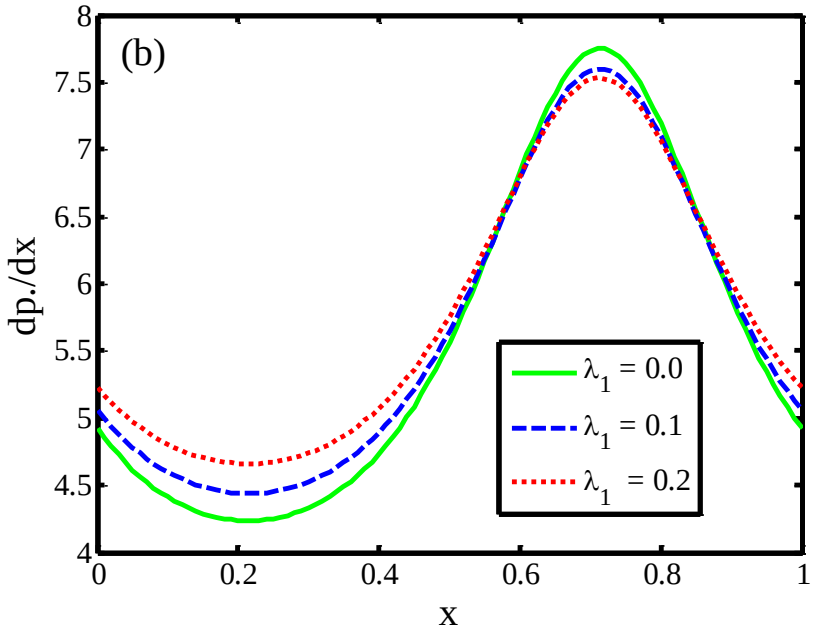
(b)
dp./dx
x
λ1 = 0.0
λ1 = 0.1
λ1 = 0.2
8
7.5
7
6.5
6
5.5
5
4.5
4
0
0.2
0.4
0.6
0.8
1

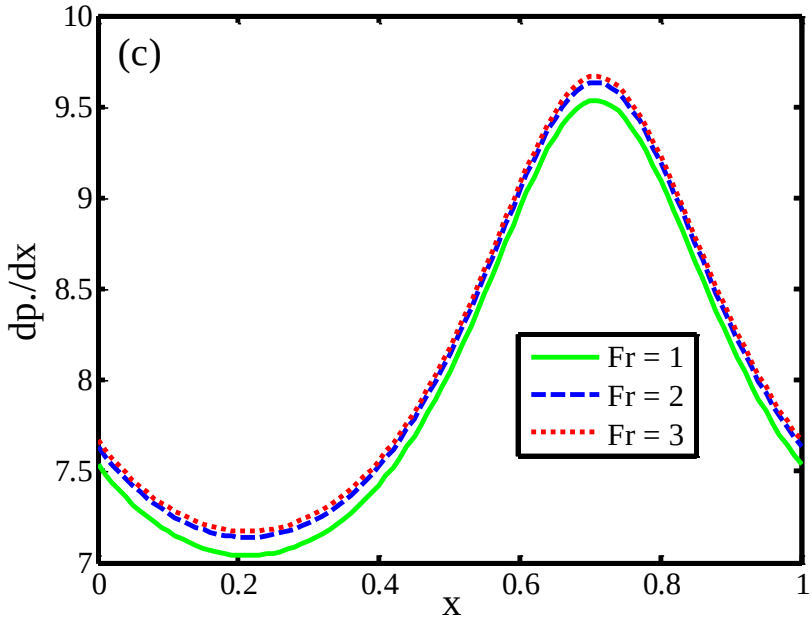
(c)
dp./dx
x
Fr = 1
Fr = 2
Fr = 3
10
9.5
9
8.5
8
7.5
7
0
0.2
0.4
0.6
0.8
1

Figure 4.

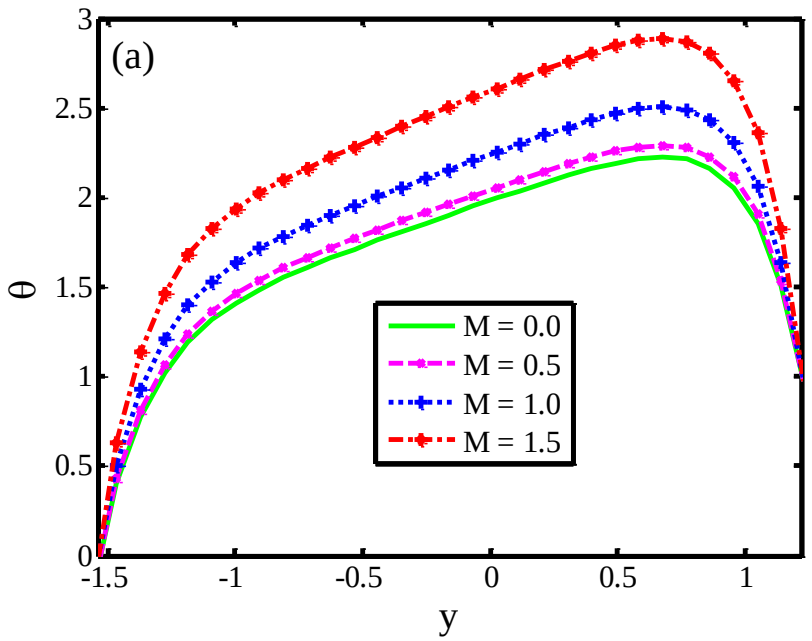
(a)
θ
y
M = 0.0
M = 0.5
M = 1.0
M = 1.5
3
2.5
2
1.5
1
0.5
0
-1.5
-1
-0.5
0
0.5
1

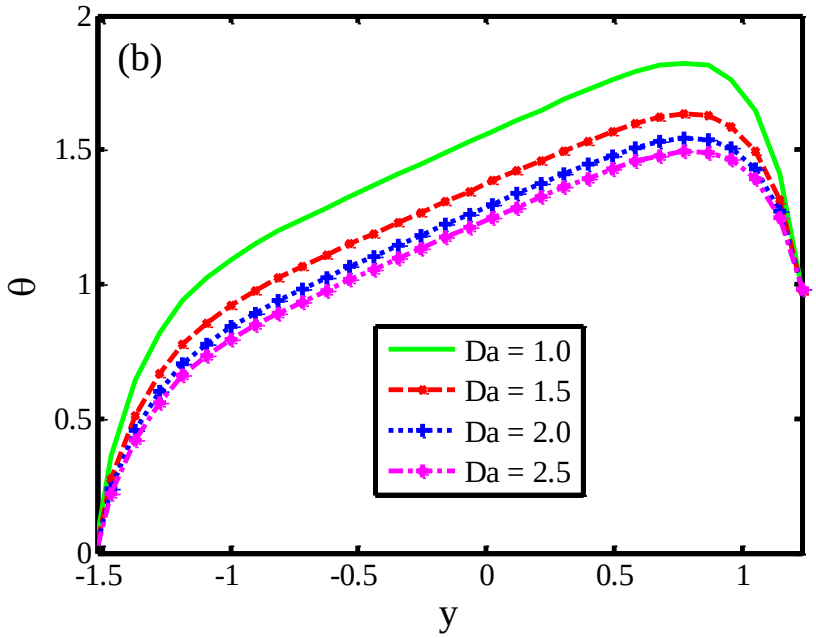
(b)
Da = 1.0
Da = 1.5
Da = 2.0
Da = 2.5
θ
y
2
1.5
1
0.5
0
-1.5
-1
-0.5
0
0.5
1

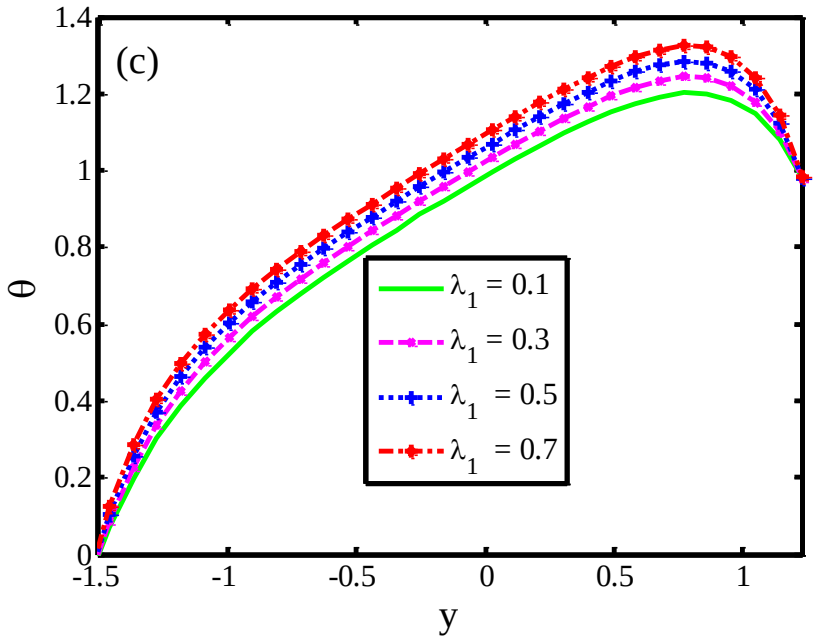
(c)
λ1 = 0.1
λ1 = 0.3
λ1 = 0.5
λ1 = 0.7
θ
y
1.4
1.2
1
0.8
0.6
0.4
0.2
0
-1.5
-1
-0.5
0
0.5
1

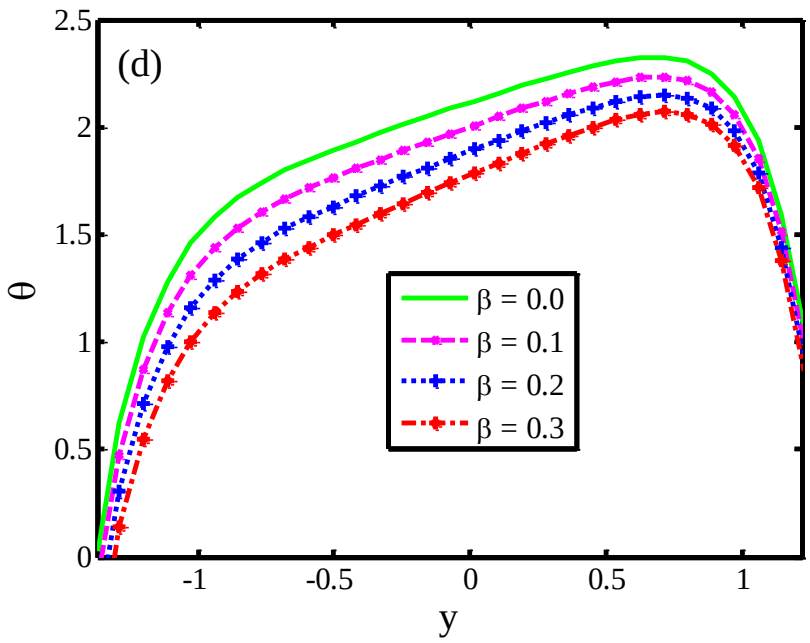
(d)
β = 0.0
β = 0.1
β = 0.2
β = 0.3
θ
y
2.5
2
1.5
1
0.5
0
-1
-0.5
0
0.5
1

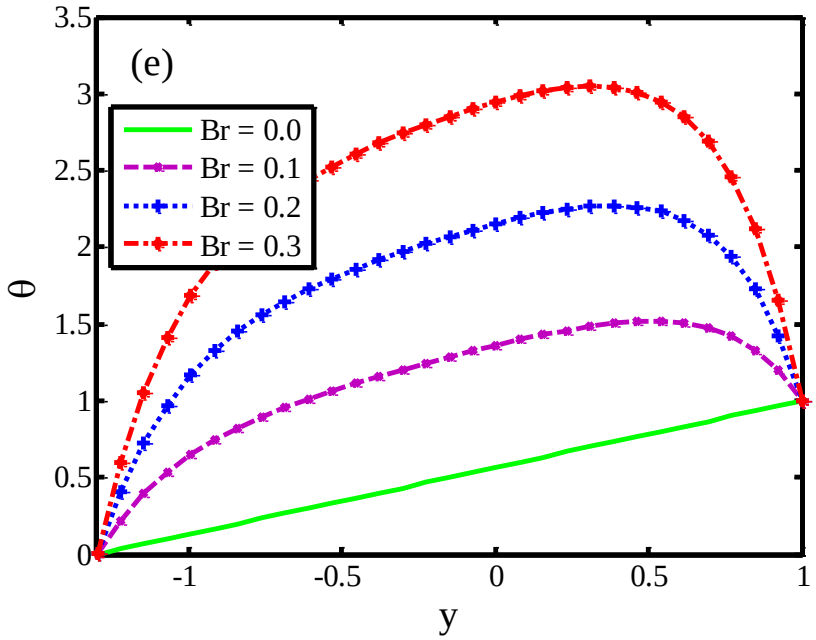
(e)
Br = 0.0
Br = 0.1
Br = 0.2
Br = 0.3
θ
y
3.5
3
2.5
2
1.5
1
0.5
0
-1
-0.5
0
0.5
1

Figure 5.

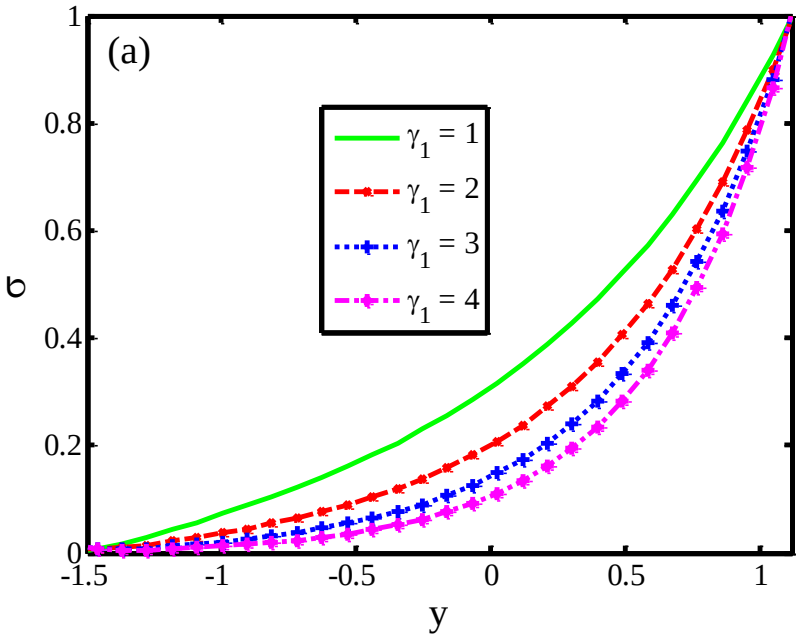
(a)
γ_1 = 1
γ_1 = 2
γ_1 = 3
γ_1 = 4
σ
y
1
0.8
0.6
0.4
0.2
0
-1.5
-1
-0.5
0
0.5
1

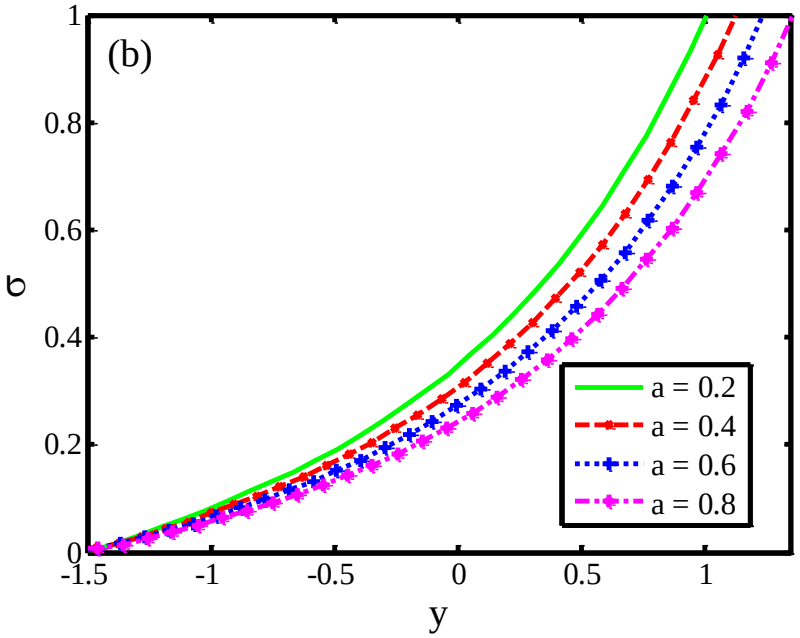
(b)
a = 0.2
a = 0.4
a = 0.6
a = 0.8
σ
y
1
0.8
0.6
0.4
0.2
0
-1.5
-1
-0.5
0
0.5
1

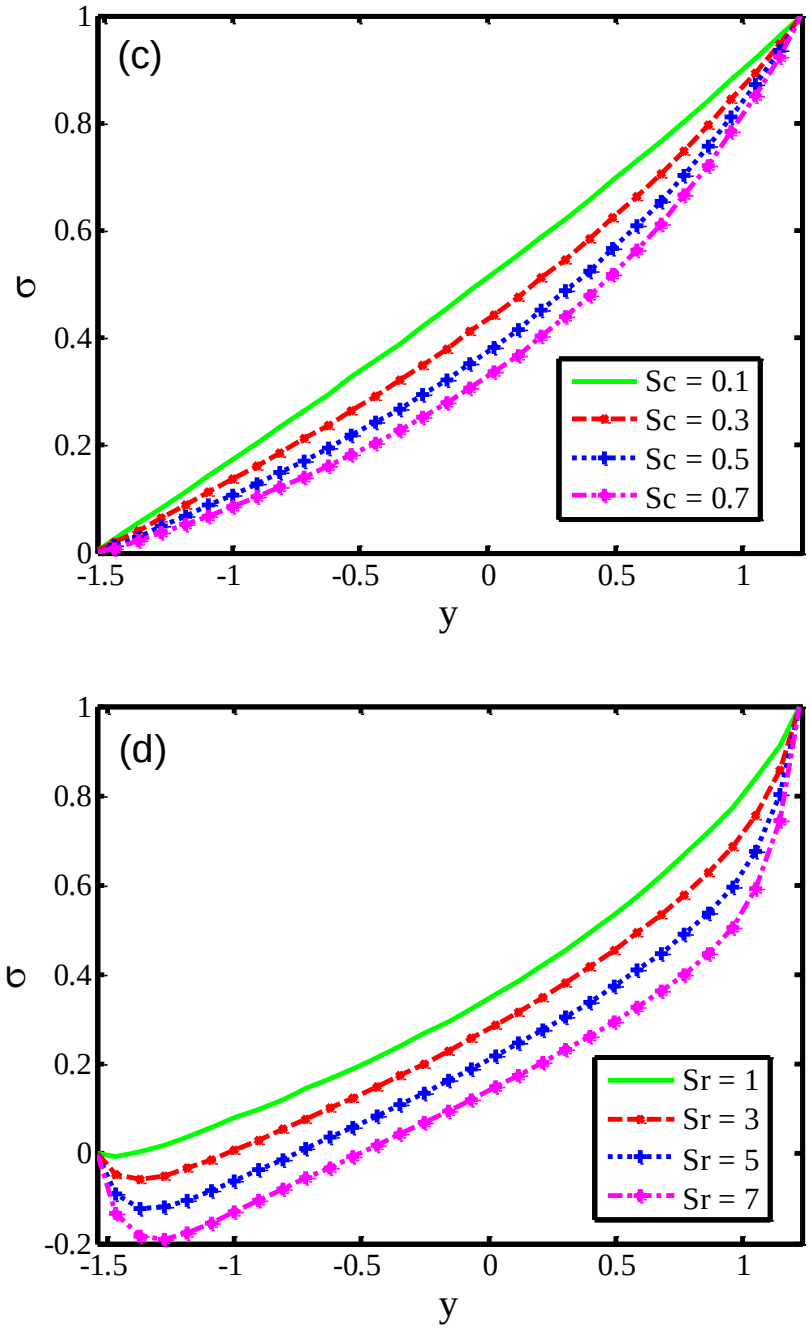

Figure 6.

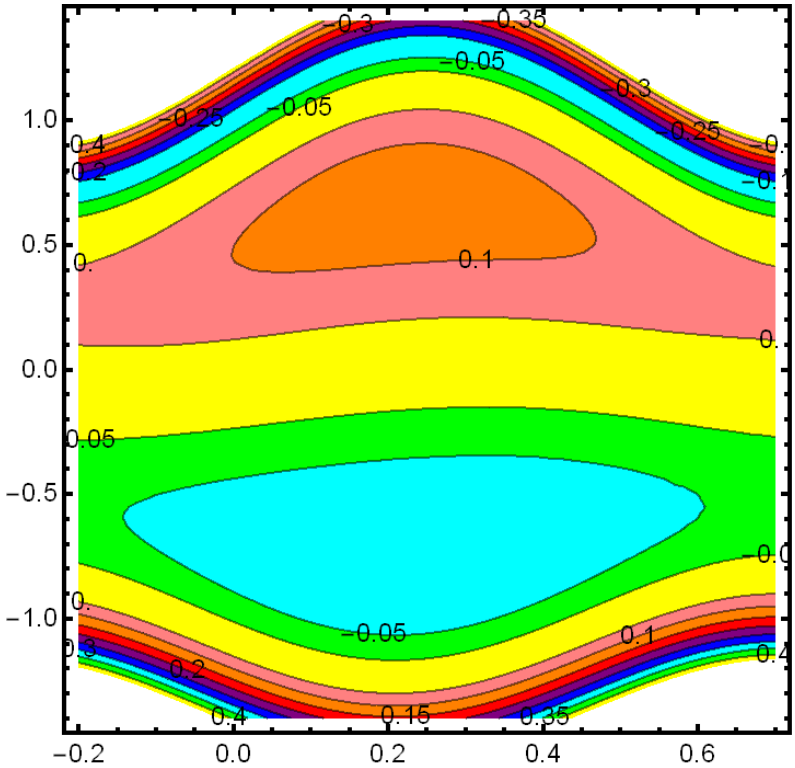
1.0
0.5
0.0
−0.5
−1.0
−0.2
0.0
0.2
0.4
0.6
−0.3
0.35
−0.05
−0.25
0.1
0.05
0.2
0.4
0.15

(a)

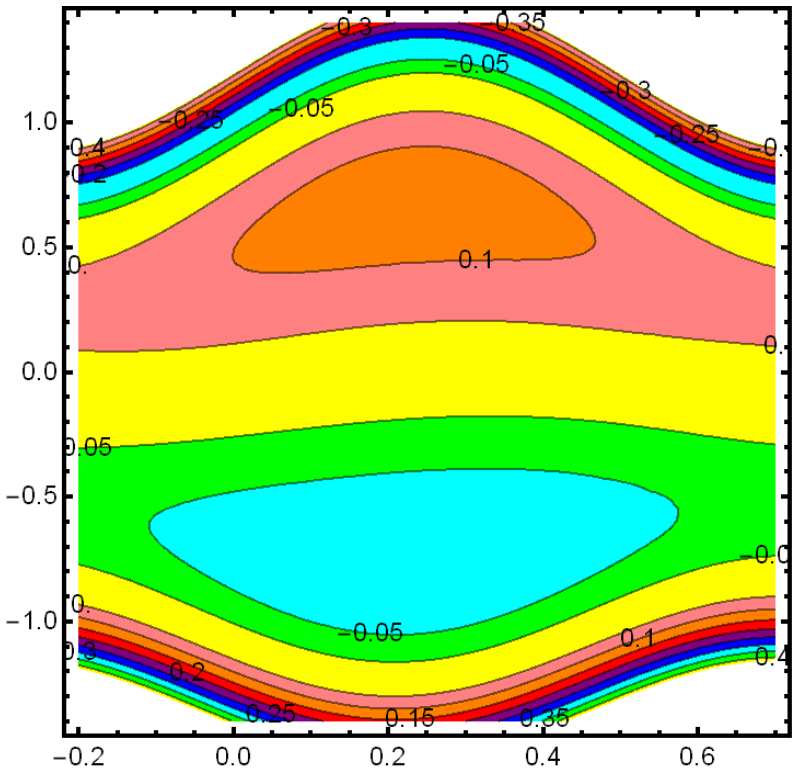
1.0
0.5
0.0
−0.5
−1.0
−0.2
0.0
0.2
0.4
0.6
−0.3
0.35
−0.05
−0.25
0.1
0.05
0.2
0.25
0.15

(b)

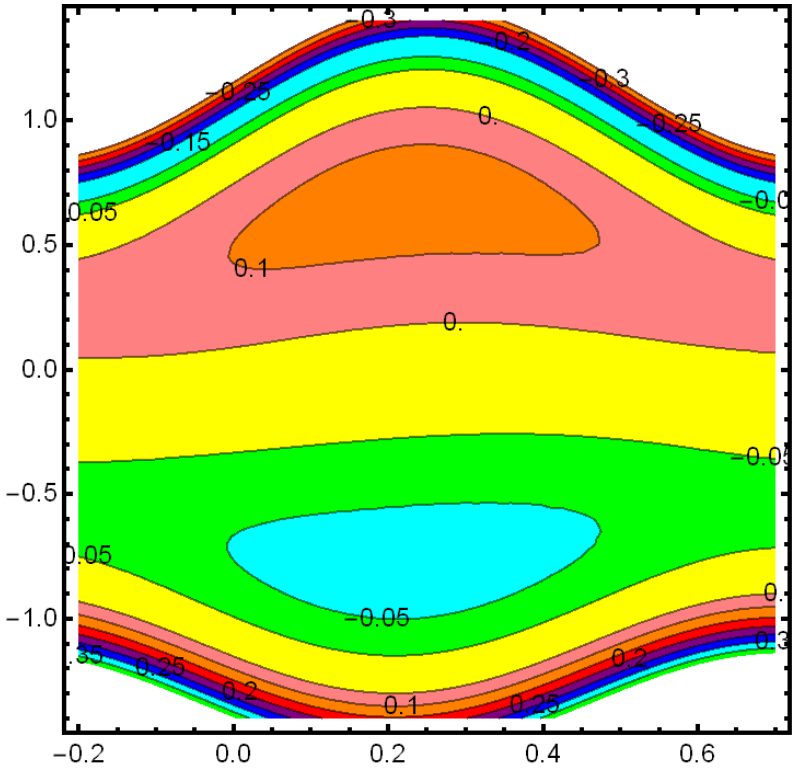
1.0
0.5
0.0
−0.5
−1.0
−0.2
0.0
0.2
0.4
0.6
0.1
0.2
0.25
0.3
−0.05
−0.15
−0.25

(c)

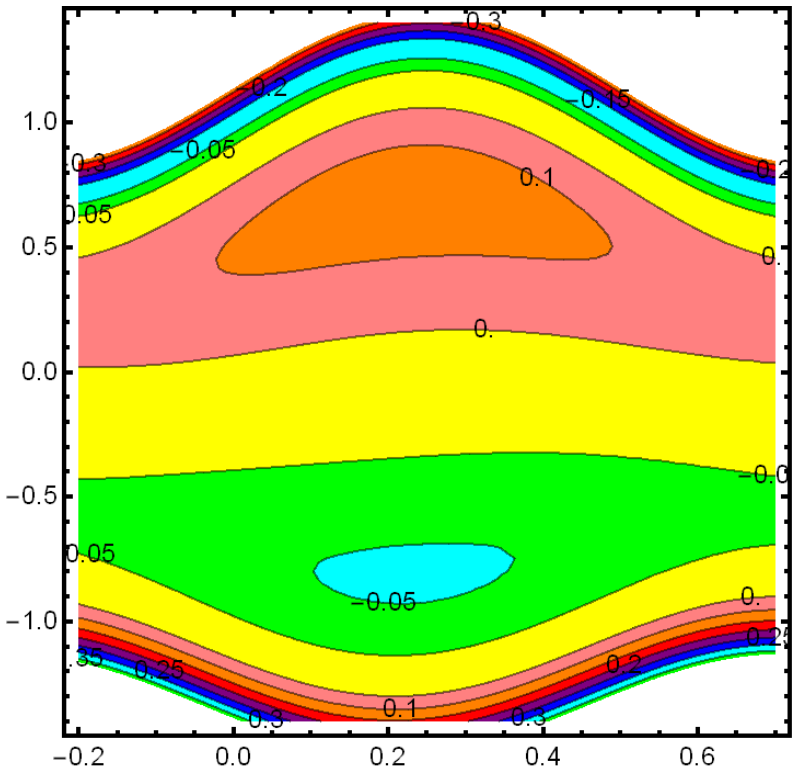
1.0
0.5
0.0
−0.5
−1.0
−0.2
0.0
0.2
0.4
0.6
0.1
0.2
0.25
0.3
−0.05
−0.15

(d)

Figure 7

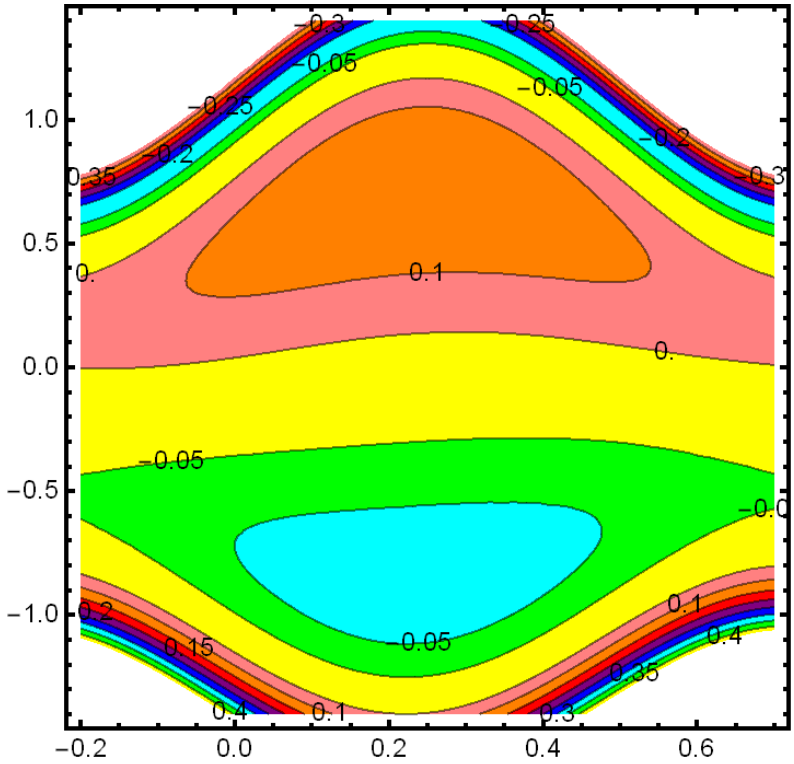
1.0
0.5
0.0
−0.5
−1.0
−0.2
0.0
0.2
0.4
0.6
−0.3
−0.25
−0.05
−0.2
0.35
0.1
0.
0.15
0.4
0.3

(a)

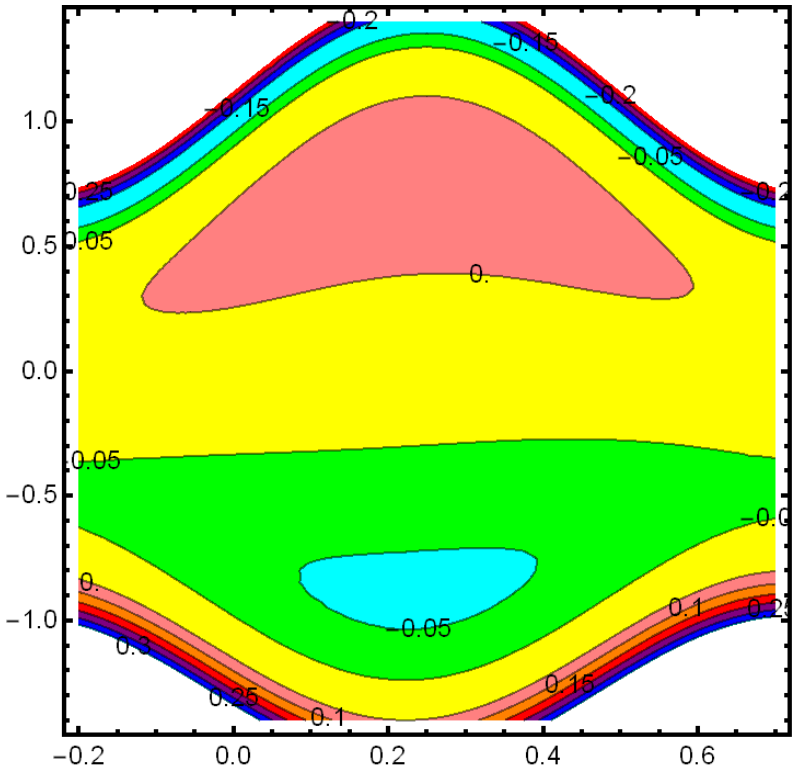
1.0
0.5
0.0
−0.5
−1.0
−0.2
0.0
0.2
0.4
0.6
0.2
−0.15
−0.05
0.25
0.05
0.
0.1
0.3
0.15

(b)

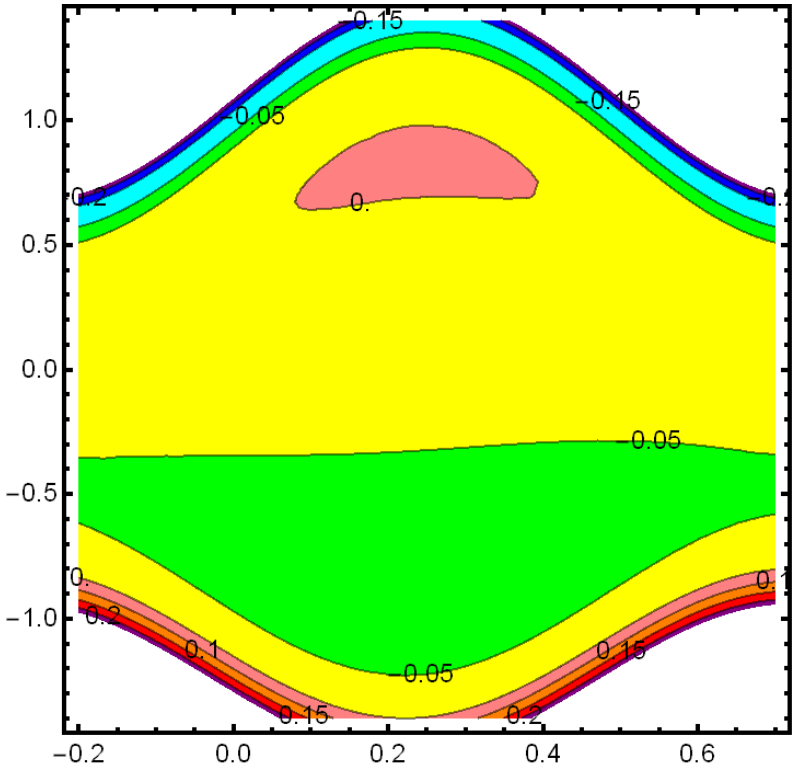
1.0
0.5
0.0
−0.5
−1.0
−0.2
0.0
0.2
0.4
0.6
−0.15
−0.05
0.05
0.1
0.15
0.2
0.

(c)

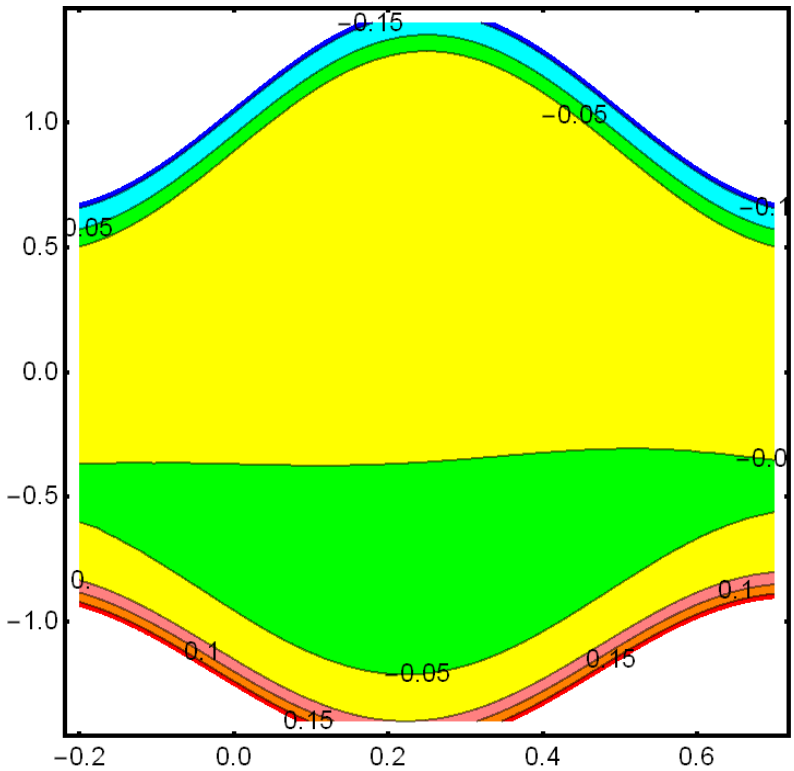
1.0
0.5
0.0
−0.5
−1.0
−0.2
0.0
0.2
0.4
0.6
−0.15
−0.05
0.05
0.1
0.15
0.

(d)

Figure 8.

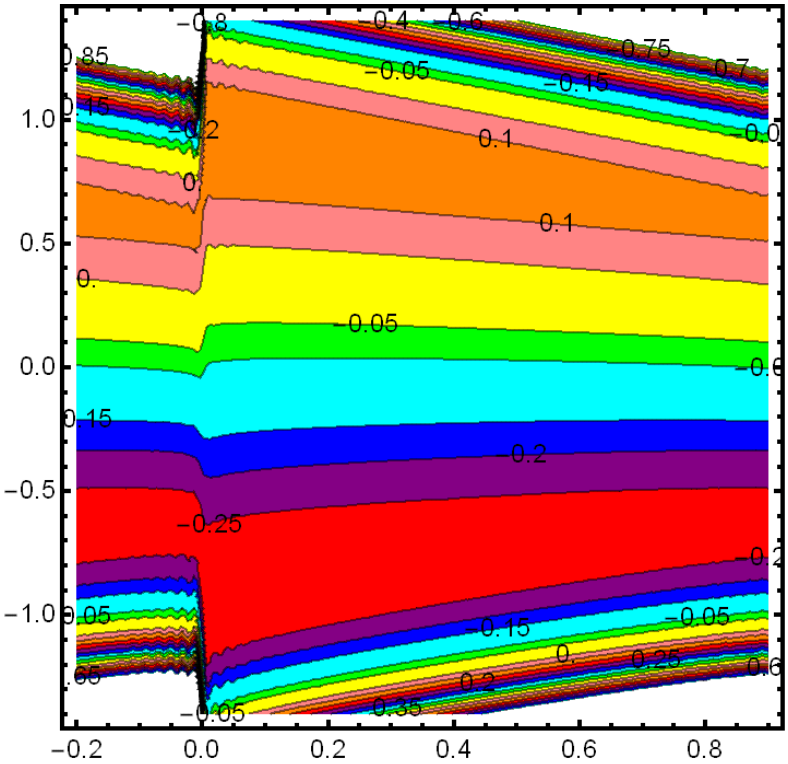

(a)

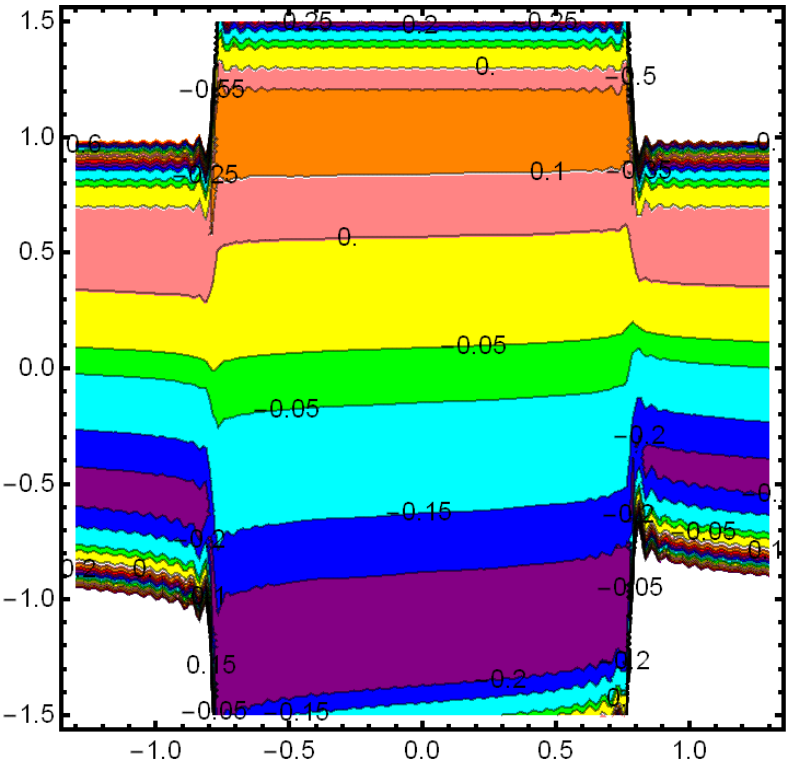

(b)

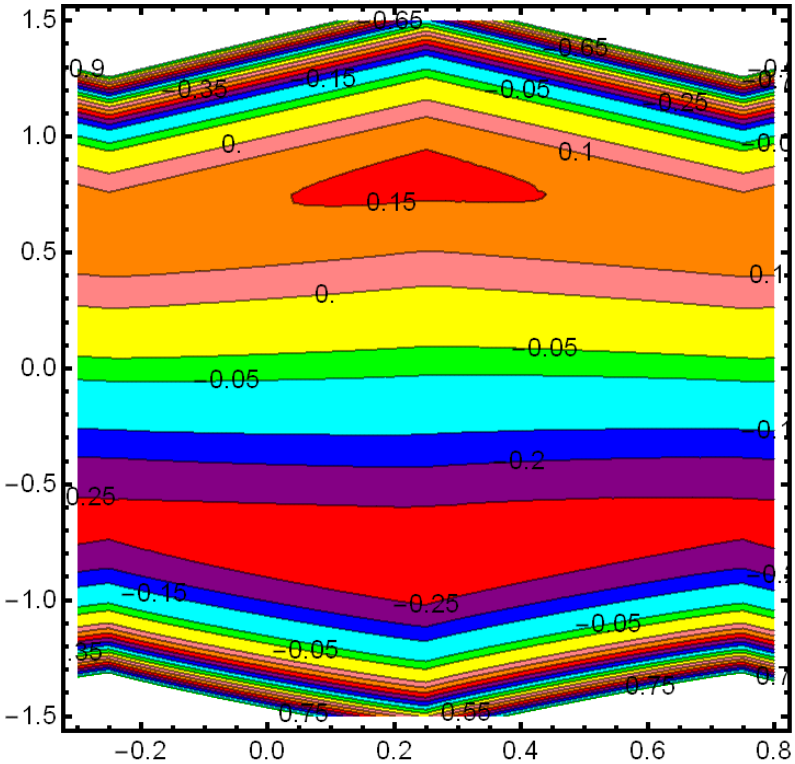
1.5
1.0
0.5
0.0
−0.5
−1.0
−1.5
−0.2
0.0
0.2
0.4
0.6
0.8
0.65
0.9
0.35
0.15
0.05
0.25
0.1
0.15
0.2
0.25
0.15
0.25
0.05
0.75
0.55

(c)

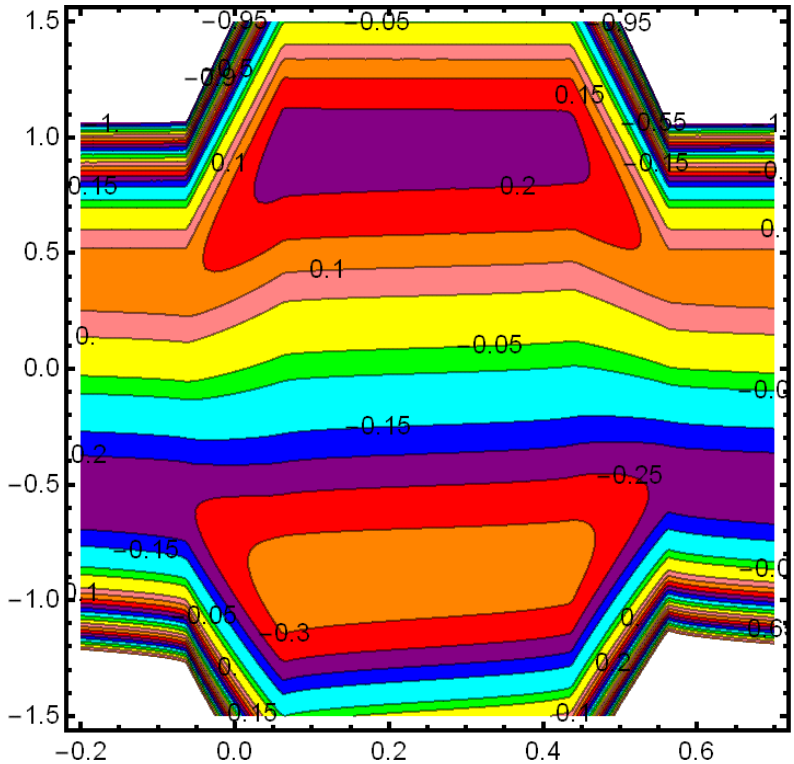
1.5
1.0
0.5
0.0
−0.5
−1.0
−1.5
−0.2
0.0
0.2
0.4
0.6
0.95
0.05
0.15
0.55
0.1
0.2
0.1
0.05
0.15
0.25
0.3

(d)

Figure 9

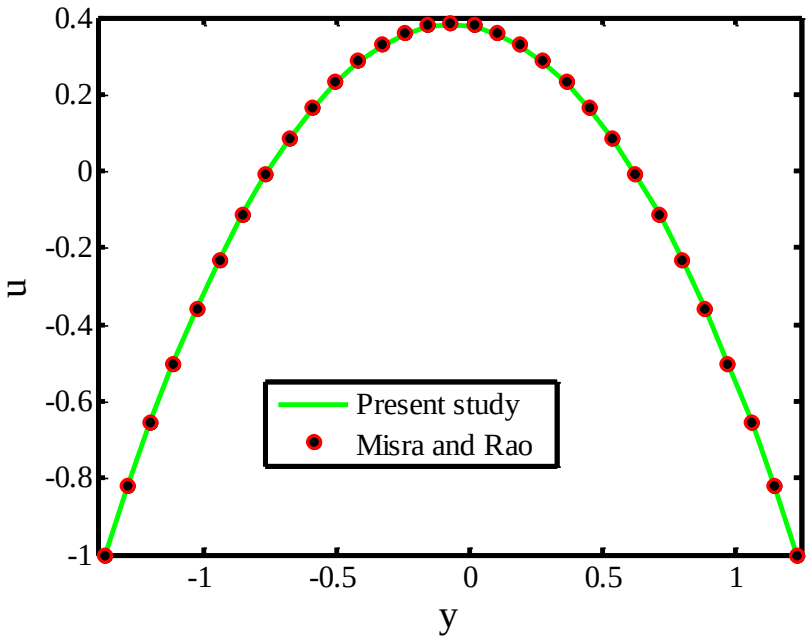

Figure 10

Biographies

Dr. R. Vijayaragavan is working as a Professor of Mathematics, Thirvalluvar University, Vellore, Tamilandu, India. He obtained his M.Sc, M.Phil and Ph.D degrees from University of Madras. He published many papers in the reputed international journals. His area of interest is computational fluid dynamics.

Dr. P. Tamizharasi is working as Assistant Professor of Mathematics, Easwari Engineering College, Ramapuram, Chennai. She obtained her M.Sc, M.Phil and Ph.D in Thiruvalluvar University, Vellore, India. Area of her research interest is Fluid dynamics especially peristaltic transport, Heat and mass transfer, nanofluid. She published more than 10 papers in the reputed international Journals.

Dr. A. Magesh is working as Assistant Professor in the department of Mathematics, Sri Sai Ram Engineering College, West Tambaram, Chennai, Tamilnadu, India. He obtained his M.Sc and M.Phil in Thiruvalluvar University and Ph.D from Anna University, Chennai, India. His area of interest is computational fluid dynamics, particularly curved channel, heat and

mass transfer, electroosmosis, porous media etc., He published more than 15 papers in the reputed international Journals. He is the reviewer of some reputed international journals.